Science Advances
AAAS

advances.sciencemag.org/cgi/content/full/4/10/eaat6533/DC1

# Supplementary Materials for

## Photonic implementation of Majorana-based Berry phases

Jin Shi Xu, Kai Sun, Jiannis K. Pachos, Yong-Jian Han*, Chuan-Feng Li*, Guang-Can Guo

*Corresponding author. Email: smhan@ustc.edu.cn (Y.-J.H.); cfli@ustc.edu.cn (C.-F.L.)

Published 19 October 2018, *Sci. Adv.* **4**, eaat6533 (2018)
DOI: 10.1126/sciadv.aat6533

**This PDF file includes:**

## Section S1. Theoretical details

### A. Principle of the imaginary time evolution

Here we explain in detail the basic idea of the imaginary time evolution (ITE) algorithm based on the cooling algorithm [38]. Each ITE operator can be realised by this method. A ITE operator can be successfully realised by a set of basic steps with some probability, which depends on the Hamiltonian and the initial state. Fortunately, in the braiding process for the KCM, the ITE operator can be efficiently realised.

The circuit for one step of the imaginary time evolution is shown in Figure S1. The key

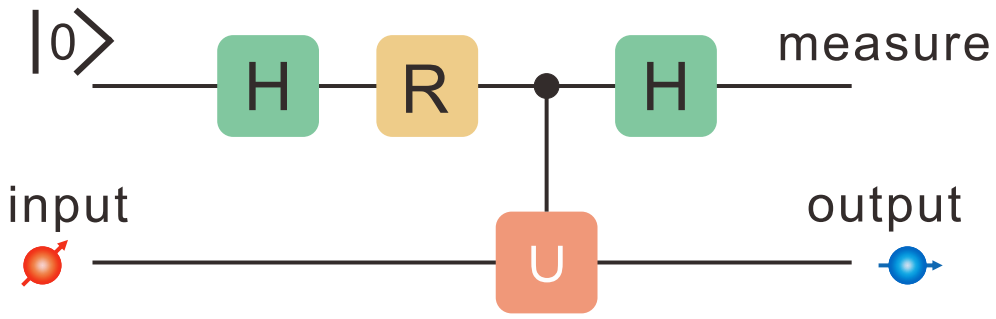


Fig. S1. (Color online). The circuit of one-step cooling algorithm. **H** represents the Hadamard gate operation. **R** represents a local phase gate and **U** is the unitary operation which is dependent on the Hamiltonian $H_s$.

components of the quantum circuit consists of four gates [38]: (a) two Hadamard gates

$$\mathsf{H} \equiv \tfrac{1}{\sqrt{2}} \left( |0\rangle + |1\rangle \right) \langle 0| + \tfrac{1}{\sqrt{2}} \left( |0\rangle - |1\rangle \right) \langle 1| \ , \tag{1}$$

applying to the ancilla qubit ($|0\rangle$ and $|1\rangle$ are the corresponding two levels) at the beginning and at the end of the quantum circuit; (b) a local phase gate,

$$\mathsf{R}_{\mathsf{z}} \left( \alpha \right) \equiv |0\rangle \langle 0| - i e^{i\alpha} |1\rangle \langle 1| \ , \tag{2}$$

where the parameter $\alpha$ is chosen to optimize the efficiency of the algorithm; (c) a two-qubit controlled unitary operation,

$$\mathbb{1} \otimes |0\rangle \langle 0| + U \otimes |1\rangle \langle 1| \ , \tag{3}$$

where $\mathbb{1}$ is the identity operator, and

$$U \left( t \right) = e^{-iH_s t} \tag{4}$$

is the real time evolution operator for the system. $H_s$ is the Hamiltonian of the considered system ($L$-site KCM here), and $t$ is the time of evolution, which is another parameter we can use to optimise the efficiency of the algorithm. For a many-body Hamiltonian, we can approximate well the unitary evolution operator $U(t)$ by the product of a set of local unitary operators through Trotter-Suzuki expansion [39].

For any given initial state of the system, $|\psi_{in}\rangle = \sum_{k=1}^{N_s} \sqrt{p_k} \sum_{l=1}^{n_k} \beta_{k,l} |e_{k,l}\rangle$, where $N_s$ is the number of the eigenvector subspace of Hamiltonian $H_s$, $n_k$ ($\sum_{k=1}^{N_s} n_k = 2^L$) is the degeneracy of the $k$-th eigenvector subspace of the Hamiltonian $H_s$ with eigenvalue $E_k$, and $|e_{k,l}\rangle$ is the $l$-th eigenvector in this subspace. The probability to find the state in the $k$-th eigenvector

subspace is denoted by $p_k$. For each $k$, $\sum_{l=1}^{n_k} \beta_{k,l} |e_{k,l}\rangle$ is normalised, i.e. $\sum_{l=1}^{n_k} |\beta_{k,l}|^2 = 1$. Generally, we do not need to know the exact form of $|e_{k,l}\rangle$.

The quantum circuit then produces the following output state:

$$\frac{1}{2}\sum_{k=1}^{N_s}\sqrt{p_k}(1-ie^{-i(E_kt-\alpha)})\sum_{l=1}^{n_k}\beta_{k,l}|e_{k,l}\rangle\,|0\rangle+\frac{1}{2}\sum_{k=1}^{N_s}\sqrt{p_k}(1+ie^{-i(E_kt-\alpha)})\sum_{l=1}^{n_k}\beta_{k,l}|e_{k,l}\rangle\,|1\rangle\,. \quad (5)$$

A measurement on the ancilla qubit in the computational basis $\{|0\rangle, |1\rangle\}$ yields the states

$$A_0\sum_{k=1}^{N_s}\sqrt{p_k}(1-ie^{-i(E_kt-\alpha)})\sum_{l=1}^{n_k}\beta_{k,l}|e_{k,l}\rangle, \quad (6)$$

and

$$A_1\sum_{k=1}^{N_s}\sqrt{p_k}(1+ie^{-i(E_kt-\alpha)})\sum_{l=1}^{n_k}\beta_{k,l}|e_{k,l}\rangle, \quad (7)$$

respectively, where $A_0$ ($A_1$) is the normalisation factor. It is clear that the coefficient of the eigenvector subspace is modified by the factor $(1-ie^{-i(E_kt-\alpha)})$ or $(1+ie^{-i(E_kt-\alpha)})$ depending on the results of the ancilla qubit. As a result, the weight of the eigenvector subspace, especially the weight of the ground-state subspace, will be modified. To clarify this point, let us consider the module of the factor $(1 \pm ie^{-i(E_kt-\alpha)})$,

$$|(1 \pm ie^{-i(E_kt-\alpha)})|^2 = 2\left[1 \pm \sin(E_kt-\alpha)\right]. \quad (8)$$

If the parameters $\alpha$ and $t$ are properly chosen, such that,

$$-\pi/2 \leq E_kt-\alpha \leq \pi/2, \quad (9)$$

for all the eigenvalue $E_k$, the function $\sin(E_kt-\alpha)$ will increase with the energy. Therefore, $1-\sin(E_kt-\alpha)$ $(1+\sin(E_kt-\alpha))$ will decrease (increase) with the increase of the eigenvalue. As a result, the weight of ground state of the system will increase along with the measurement result $|0\rangle$ on the ancilla qubit, and the weight of the ground state will decrease along with the measurement result $|1\rangle$ on the ancilla qubit.

To make the parameters satisfy the condition introduced above, we normalise the Hamiltonian of the system to make the eigenvalues of the Hamiltonian to be within the range $[-1, 1]$. The general Hamiltonian in our braiding processes of MZMs in the $L$-site KCM can be easily normalised as

$$H' = \frac{i}{L}[\sum_{j=1}^{m}\frac{1}{2}\gamma_{2j-1}\gamma_{2j} + \sum_{j=m+1}^{L}\gamma_{2j}\gamma_{2j+1}]. \quad (10)$$

By setting $\alpha = 0$ and supposing the parameter $t$ satisfies the condition: $E_k t \ll 1$, the weight of the eigenvectors of the Hamiltonian change as

$$1 - \sin(E_k t) \approx e^{-E_k t}, \tag{11}$$

which is the imaginary time evolution operator for small time $t$.

To realise an ITE with a large $t$, we divide it into $k$ steps, where each step satisfies the condition introduced before. Thus, a total of $k$ steps of ITE are applied on the initial state (we make no measurement during the cooling; we measure the qubits at the end of the manipulation). The final state we obtain is

$$|\psi_{fin}\rangle = \sum_{j=0}^{k} \sqrt{C_k^j} \Big( \sum_{i=1}^{N_s} \sqrt{p_i (1/2 + a_i)^{k-j} (1/2 - a_i)^j} \sum_{l=1}^{n_i} \beta_{i,l} |e_{i,l}\rangle |\varphi_{ji}\rangle \Big), \tag{12}$$

where $|\varphi_{ji}\rangle$ is a properly normalised state of the ancilla. $a_i = \frac{1}{2}\sin(E_i t - \alpha)$ and $\alpha = 0$. After the manipulations, we measure the ancilla. The probability to get $j$ $|0\rangle$ (the number of the success cooling manipulation) is,

$$C_k^j \sum_{i=1}^{2^n} p_i (1/2 + a_i)^{k-j} (1/2 - a_i)^j. \tag{13}$$

This is a mixture of several binomial distributions with the first one corresponding to the ground state. For a standard binomial distribution: $C_k^j p^j (1-p)^{k-j}$, the expected value is $kp$ and the variance is $np(1-p)$. Thus, the concentration interval of the binomial distribution is between $k((\frac{1}{2} - a_i) - \frac{1}{\sqrt{k}}\sqrt{\frac{1}{4} - a_i^2})$ and $k((\frac{1}{2} - a_i) + \frac{1}{\sqrt{k}}\sqrt{\frac{1}{4} - a_i^2})$. In order to prepare the ground state of the system, the intersection between different binomial distribution should be very small. In other words

$$k((\frac{1}{2} - a_1) - \frac{1}{\sqrt{k}}\sqrt{\frac{1}{4} - a_1^2}) \gg k((\frac{1}{2} - a_2) + \frac{1}{\sqrt{k}}\sqrt{\frac{1}{4} - a_2^2}), \tag{14}$$

which is equivalent to

$$\sqrt{k}(a_2 - a_1) \gg \frac{1}{2} - (a_1^2 + a_2^2). \tag{15}$$

It should be noted that the other binomial distribution corresponding to higher energy have much less intersection with the distribution corresponding to ground states. Under the condition $E_k t \ll 1$ ($k = 1, 2, \cdots, 2^L$), we have

$$\frac{1}{2} - (a_1^2 + a_2^2) \approx \frac{1}{2}, a_2 - a_1 \approx \frac{1}{2}\Delta t, \tag{16}$$

and the intersection condition can be simplified to

$$\sqrt{k}\Delta t \gg 1, \tag{17}$$

where $\Delta$ is the gap of the system. If this condition is satisfied, the binomial distribution of the ground state is sufficiently separated from the others, and the number of $|0\rangle$ outcomes during the measurement on the ancilla will be concentrated at $k(1-\frac{1}{2}a_1)$ with probability $p_1$. Thus, the number of measurements that successfully obtain the ground state of the system scale as

$$\frac{1}{p_1(\Delta t)^2}. \tag{18}$$

The gap of the Hamiltonian during the braiding increases polynomially with $L$. In addition, the overlap between the ground state of $H_i^{MF}$ and $H_{i+1}^{MF}$ is independent of $L$. Therefore, the ITE operator $e^{-H_i t}$ with large $t$ is a polynomial of $L$ in the KCM Braiding situation.

### B. The state evolution during the exchange of MZMs A and C

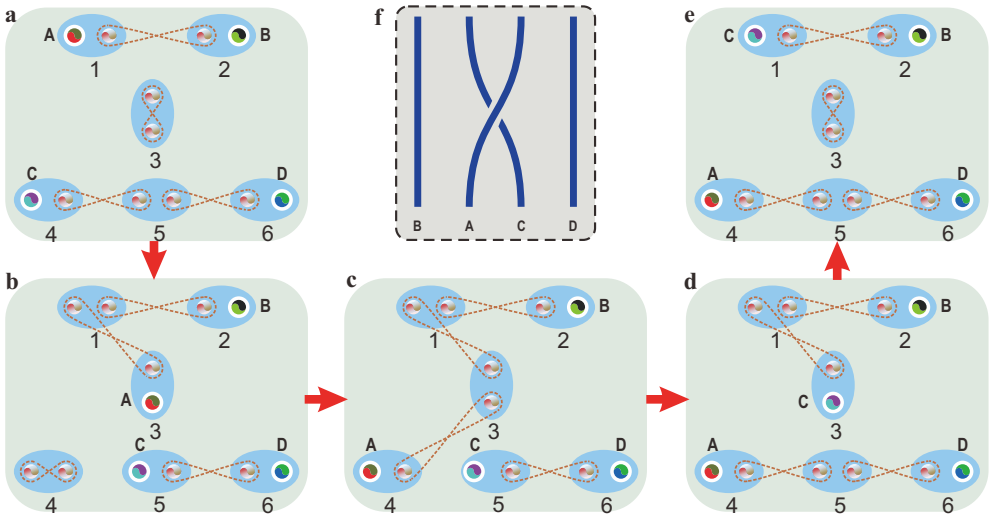


Fig. S2. The process of anticlockwise braiding of MZMs A and C. The Kitaev chains consist of six fermions (numbered from 1 to 6) with four isolated endpoint MZMs A, B, C and D. Each two particles in the blue ellipse form a conventional fermion. The dashed lines between different Majorana fermions ($k$ and $l$= $1a, 1b, \cdots, 6b$) represent the interactions, $i\gamma_k\gamma_l$, between them. **a**, **b**, **c**, **d** and **e** correspond to the imaginary-time evolution corresponding to the Hamiltonians of $H_0$, $H_1$, $H_2$, $H_3$ and $H_0$, respectively. **f.** The worldline strands corresponding to the anticlockwise braiding.

The process to anticlockwise braid Majorana zero modes (MZMs) A and C is described

in Fig. S2. The exchange process is controlled by four Hamiltonians

$$\begin{aligned} H_{M_0} &= i(\gamma_{1b}\gamma_{2a} + \gamma_{4b}\gamma_{5a} + \gamma_{5b}\gamma_{6a}) + i\gamma_{3a}\gamma_{3b}, \\ H_{h_1} &= i(\gamma_{1b}\gamma_{2a} + \gamma_{1a}\gamma_{3a} + \gamma_{5b}\gamma_{6a}) + i\gamma_{4a}\gamma_{4b}, \\ H_{h_2} &= i(\gamma_{1b}\gamma_{2a} + \gamma_{1a}\gamma_{3a} + \gamma_{3b}\gamma_{4b} + \gamma_{5b}\gamma_{6a}), \\ H_{h_3} &= i(\gamma_{1b}\gamma_{2a} + \gamma_{1a}\gamma_{3a} + \gamma_{4b}\gamma_{5a} + \gamma_{5b}\gamma_{6a}). \end{aligned} \tag{19}$$

The consecutive Hamiltonians are adiabatically connected and $H_{h_3}$ is finally adiabatically evolved to the initial Hamiltonian $H_{M_0}$. The adiabatic transport of the MZMs is implemented with our photonic simulator by imaginary-time evolution (ITE) operators [25].

Under the Jordan-Wigner (JW) transformation, the fermionic Hamiltonians $H_{M_0}$, $H_{h_1}$, $H_{h_2}$ and $H_{h_3}$ can be transformed to the corresponding spin Hamiltonians $H_0$, $H_1$, $H_2$ and $H_3$, respectively, where

$$\begin{aligned} H_0 &= -\sigma_1^x\sigma_2^x + \sigma_3^z - \sigma_4^x\sigma_5^x - \sigma_5^x\sigma_6^x, \\ H_1 &= -\sigma_1^x\sigma_2^x + \sigma_1^y\sigma_2^z\sigma_3^x + \sigma_4^z - \sigma_5^x\sigma_6^x, \\ H_2 &= -\sigma_1^x\sigma_2^x + \sigma_1^y\sigma_2^z\sigma_3^x + \sigma_3^x\sigma_4^y - \sigma_5^x\sigma_6^x, \\ H_3 &= -\sigma_1^x\sigma_2^x + \sigma_1^y\sigma_2^z\sigma_3^x - \sigma_4^x\sigma_5^x - \sigma_5^x\sigma_6^x. \end{aligned} \tag{20}$$

The JW transformation between the fermionic and spin Hamiltonians preserves their spectrum. So the adiabatic transport of the fermions system can be studied in the corresponding spin description. We can further simplify the process of ITE as many of the terms in $H_0$, $H_1$, $H_2$ and $H_3$ commute with each other. The ground states of the corresponding Hamiltonians can be expressed in terms of the eigenvectors $\{|x\rangle, |\bar{x}\rangle\}$, $\{|y\rangle, |\bar{y}\rangle\}$ and $\{|z\rangle, |\bar{z}\rangle\}$ of the corresponding Pauli operators $\sigma^x$, $\sigma^y$ and $\sigma^z$, with eigenvalues $\{1, -1\}$, respectively. The detailed evolution in the spin system during the exchange is calculated as follows.

After the ITE of the initial Hamiltonian

$$H_0 = -\sigma_1^x\sigma_2^x + \sigma_3^z - \sigma_4^x\sigma_5^x - \sigma_5^x\sigma_6^x, \tag{21}$$

which corresponds to creating the MZMs A, B, C and D, the state becomes

$$|\phi_0\rangle = \alpha|x_1x_2\bar{z}_3x_4x_5x_6\rangle + \beta|\bar{x}_1\bar{x}_2\bar{z}_3x_4x_5x_6\rangle + \mu|x_1x_2\bar{z}_3\bar{x}_4\bar{x}_5\bar{x}_6\rangle + \nu|\bar{x}_1\bar{x}_2\bar{z}_3\bar{x}_4\bar{x}_5\bar{x}_6\rangle, \tag{22}$$

where $\alpha$, $\beta$, $\mu$ and $\nu$ are complex amplitudes satisfying $|\alpha|^2 + |\beta|^2 + |\mu|^2 + |\nu|^2 = 1$.

Then, the state $|\phi_0\rangle$ is sent to the ITE operation of the second Hamiltonian

$$H_1 = -\sigma_1^x\sigma_2^x + \sigma_1^y\sigma_2^z\sigma_3^x + \sigma_4^z - \sigma_5^x\sigma_6^x, \tag{23}$$

which corresponds to transporting the MZM A to site 3 and MZM C to site 5. The Hamiltonians $H_0$ and $H_1$ share the terms $-\sigma_1^x\sigma_2^x$ and $-\sigma_5^x\sigma_6^x$. Therefore, we only implement the additional ITE operations of $\sigma_4^z$ and $\sigma_1^y\sigma_2^z\sigma_3^x$. Then the output state becomes

$$\begin{aligned}
|\phi_1\rangle = &[\alpha(1+i)+\beta(1-i)]|\bar{y}_1 z_2 x_3 \bar{z}_4 x_5 x_6\rangle \\
&+[-\alpha(1+i)+\beta(1-i)]|\bar{y}_1 \bar{z}_2 \bar{x}_3 \bar{z}_4 x_5 x_6\rangle \\
&+[\alpha(1-i)-\beta(1+i)]|y_1 \bar{z}_2 x_3 \bar{z}_4 x_5 x_6\rangle \\
&+[-\alpha(1-i)-\beta(1+i)]|y_1 z_2 \bar{x}_3 \bar{z}_4 x_5 x_6\rangle \\
&+[-\mu(1+i)-\nu(1-i)]|\bar{y}_1 z_2 x_3 \bar{z}_4 \bar{x}_5 \bar{x}_6\rangle \\
&+[\mu(1+i)-\nu(1-i)]|\bar{y}_1 \bar{z}_2 \bar{x}_3 \bar{z}_4 \bar{x}_5 \bar{x}_6\rangle \\
&+[-\mu(1-i)+\nu(1+i)]|y_1 \bar{z}_2 x_3 \bar{z}_4 \bar{x}_5 \bar{x}_6\rangle \\
&+[\mu(1-i)+\nu(1+i)]|y_1 z_2 \bar{x}_3 \bar{z}_4 \bar{x}_5 \bar{x}_6\rangle.
\end{aligned} \tag{24}$$

Subsequently, the state $|\phi_1\rangle$ is sent to the ITE operation of the third Hamiltonian

$$H_2 = -\sigma_1^x\sigma_2^x + \sigma_1^y\sigma_2^z\sigma_3^x + \sigma_3^x\sigma_4^y - \sigma_5^x\sigma_6^x, \tag{25}$$

which corresponds to transporting MZM A to site 4. We need only consider the ITE operation of $\sigma_3^x\sigma_4^y$ giving the output state

$$\begin{aligned}
|\phi_2\rangle = &[\alpha(1+i)+\beta(1-i)]|\bar{y}_1 z_2 x_3 \bar{y}_4 x_5 x_6\rangle \\
&-[-\alpha(1+i)+\beta(1-i)]|\bar{y}_1 \bar{z}_2 \bar{x}_3 y_4 x_5 x_6\rangle \\
&+[\alpha(1-i)-\beta(1+i)]|y_1 \bar{z}_2 x_3 \bar{y}_4 x_5 x_6\rangle \\
&-[-\alpha(1-i)-\beta(1+i)]|y_1 z_2 \bar{x}_3 y_4 x_5 x_6\rangle \\
&+[-\mu(1+i)-\nu(1-i)]|\bar{y}_1 z_2 x_3 \bar{y}_4 \bar{x}_5 \bar{x}_6\rangle \\
&-[\mu(1+i)-\nu(1-i)]|\bar{y}_1 \bar{z}_2 \bar{x}_3 y_4 \bar{x}_5 \bar{x}_6\rangle \\
&+[-\mu(1-i)+\nu(1+i)]|y_1 \bar{z}_2 x_3 \bar{y}_4 \bar{x}_5 \bar{x}_6\rangle \\
&-[\mu(1-i)+\nu(1+i)]|y_1 z_2 \bar{x}_3 y_4 \bar{x}_5 \bar{x}_6\rangle.
\end{aligned} \tag{26}$$

The state $|\phi_2\rangle$ is sent to the ITE operation of the forth Hamiltonian

$$H_3 = -\sigma_1^x\sigma_2^x + \sigma_1^y\sigma_2^z\sigma_3^x - \sigma_4^x\sigma_5^x - \sigma_5^x\sigma_6^x, \tag{27}$$

which corresponds to transporting MZM C to site 3. We need only consider the ITE operation of $-\sigma_4^x\sigma_5^x$. The state becomes

$$\begin{aligned}|\phi_3\rangle = &(\alpha - i\beta)|\bar{y}_1 z_2 x_3 x_4 x_5 x_6\rangle - i(\alpha - i\beta)|y_1 \bar{z}_2 x_3 x_4 x_5 x_6\rangle \\ &+ i(\alpha + i\beta)|\bar{y}_1 \bar{z}_2 \bar{x}_3 x_4 x_5 x_6\rangle + (\alpha + i\beta)|y_1 z_2 \bar{x}_3 x_4 x_5 x_6\rangle \\ &+ i(-\mu + i\nu)|\bar{y}_1 z_2 x_3 \bar{x}_4 \bar{x}_5 \bar{x}_6\rangle + (-\mu + i\nu)|y_1 \bar{z}_2 x_3 \bar{x}_4 \bar{x}_5 \bar{x}_6\rangle \\ &- (\mu + i\nu)|\bar{y}_1 \bar{z}_2 \bar{x}_3 \bar{x}_4 \bar{x}_5 \bar{x}_6\rangle + i(\mu + i\nu)|y_1 z_2 \bar{x}_3 \bar{x}_4 \bar{x}_5 \bar{x}_6\rangle.\end{aligned} \tag{28}$$

Finally, we employ the ITE operation to move back to the initial Hamiltonian

$$H_0 = -\sigma_1^x\sigma_2^x + \sigma_3^z - \sigma_4^x\sigma_5^x - \sigma_5^x\sigma_6^x. \tag{29}$$

This operation corresponds to transporting MZM C back to site 1. For that we need to only consider the ITE operation of $\sigma_3^z$. The output state becomes

$$\begin{aligned}|\phi_3\rangle = &(\alpha - i\beta)|\bar{y}_1 z_2 \bar{z}_3 x_4 x_5 x_6\rangle - i(\alpha - i\beta)|y_1 \bar{z}_2 \bar{z}_3 x_4 x_5 x_6\rangle \\ &- i(\alpha + i\beta)|\bar{y}_1 \bar{z}_2 \bar{z}_3 x_4 x_5 x_6\rangle - (\alpha + i\beta)|y_1 z_2 \bar{z}_3 x_4 x_5 x_6\rangle \\ &+ i(-\mu + i\nu)|\bar{y}_1 z_2 \bar{z}_3 \bar{x}_4 \bar{x}_5 \bar{x}_6\rangle + (-\mu + i\nu)|y_1 \bar{z}_2 \bar{z}_3 \bar{x}_4 \bar{x}_5 \bar{x}_6\rangle \\ &+ (\mu + i\nu)|\bar{y}_1 \bar{z}_2 \bar{z}_3 \bar{x}_4 \bar{x}_5 \bar{x}_6\rangle - i(\mu + i\nu)|y_1 z_2 \bar{z}_3 \bar{x}_4 \bar{x}_5 \bar{x}_6\rangle.\end{aligned} \tag{30}$$

In order to compare this final state with the initial one, we change the basis of modes 1 and 2 to $|x\rangle$ and $|\bar{x}\rangle$ (basis rotation). The state becomes

$$\begin{aligned}|\phi_4\rangle = &(\alpha + \beta)|x_1 x_2 \bar{z}_3 x_4 x_5 x_6\rangle + (\mu - \nu)|x_1 x_2 \bar{z}_3 \bar{x}_4 \bar{x}_5 \bar{x}_6\rangle \\ &+ (\beta - \alpha)|\bar{x}_1 \bar{x}_2 \bar{z}_3 x_4 x_5 x_6\rangle + (\mu + \nu)|\bar{x}_1 \bar{x}_2 \bar{z}_3 \bar{x}_4 \bar{x}_5 \bar{x}_6\rangle.\end{aligned} \tag{31}$$

As shown in the main text, the unitary transformation that corresponds to the anticlockwise braiding of MZMs A and C reads

$$U = \frac{1}{\sqrt{2}} \begin{pmatrix} 1 & 0 & 0 & -1 \\ 0 & 1 & -1 & 0 \\ 0 & 1 & 1 & 0 \\ 1 & 0 & 0 & 1 \end{pmatrix}, \tag{32}$$

written in the basis $\{|00_g\rangle, |01_g\rangle, |10_g\rangle, |11_g\rangle\}$.

If we focus on the even fermionic parity space spanned by $|00_g\rangle$ and $|11_g\rangle$, the unitary transformation becomes

$$U = \frac{1}{\sqrt{2}} \begin{pmatrix} 1 & -1 \\ 1 & 1 \end{pmatrix}. \tag{33}$$

As a result, the braiding of A and C corresponds to a Hadamard gate operation. Note that this is not the standard Hadamard gate, which equals to $\mathrm{H}\cdot\mathrm{R}^2$. With a similar calculation, we can verify that the clockwise braiding of the MZMs A and C can be realised as shown in Fig. S3.

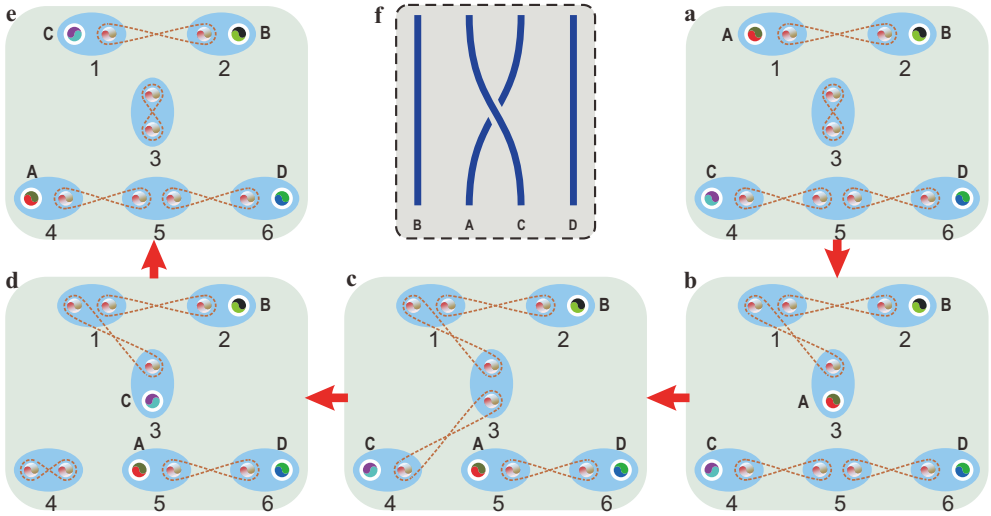


Fig. S3. The process of clockwise braiding of MZMs A and C. The Kitaev chains consist of six fermions (numbered from 1 to 6) with four isolated endpoint MZMs A, B, C and D. Each two particles in the blue ellipse form a conventional fermion. The dashed lines between different Majorana fermions ($k$ and $l$= $1a, 1b, \cdots, 6b$) represent the interactions, $i\gamma_k\gamma_l$, between them. **a**, **b**, **c**, **d** and **e** correspond to the imaginary-time evolution of the Hamiltonians similar to the clockwise braiding situation. **f.** The worldline strands of the clockwise braiding of the MZMs A and C.

### C. The state evolution during the exchange of MZMs C and D

The process to anticlockwise braiding the MZMs C and D is described in Fig. S4. With the same arguments, the braiding of the MZMs C and D can be implemented by the ITE opertors based on the following Hamiltonians

$$\begin{aligned} H_{M_0} &= i(\gamma_{1b}\gamma_{2a} + \gamma_{4b}\gamma_{5a} + \gamma_{5b}\gamma_{6a}) + i\gamma_{3a}\gamma_{3b}, \\ H_{r_1} &= i(\gamma_{1b}\gamma_{2a} + \gamma_{5b}\gamma_{6a}) + i(\gamma_{3a}\gamma_{3b} + \gamma_{4a}\gamma_{4b}), \\ H_{r_2} &= i(\gamma_{1b}\gamma_{2a} + \gamma_{4b}\gamma_{6b} + \gamma_{5b}\gamma_{6a}) + i\gamma_{3a}\gamma_{3b}. \end{aligned} \tag{34}$$

The braiding process can be simulated by the spin system with the corresponding Hamil-

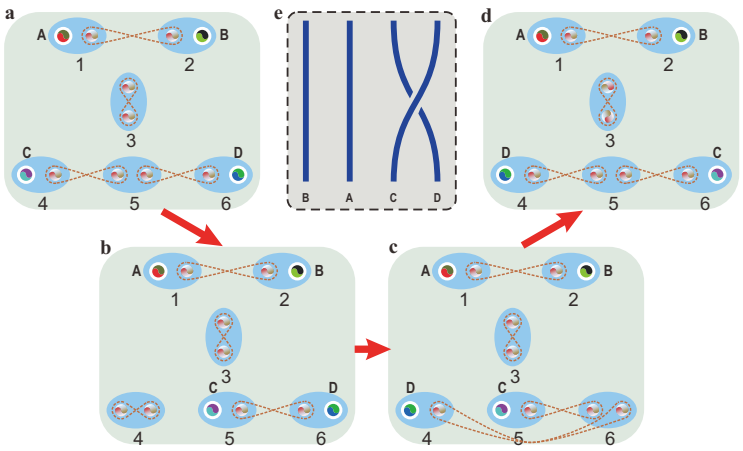


Fig. S4. The process to anticlockwise braiding of MZMs C and D. The Kitaev chains consist of six fermions (numbered from 1 to 6) with four isolated endpoint MZMs A, B, C and D. Each two particles in the blue ellipse form a conventional fermion. The dashed lines between different Majorana fermions ($k$ and $l$= $1a, 1b, \cdots, 6b$) represent the interactions, $i\gamma_k\gamma_l$, between them. **a**, **b**, **c**, **d** correspond to the imaginary-time evolution of Hamiltonian of $H_0$, $H_1'$, $H_2'$ and $H_0$, respectively. **e.** The worldline strands representing the anticlockwise braiding between the C and D MZMs.

tonians

$$\begin{aligned} H_0 &= -\sigma_1^x\sigma_2^x + \sigma_3^z - \sigma_4^x\sigma_5^x - \sigma_5^x\sigma_6^x, \\ H_1' &= -\sigma_1^x\sigma_2^x + \sigma_3^z + \sigma_4^z - \sigma_5^x\sigma_6^x, \\ H_2' &= -\sigma_1^x\sigma_2^x + \sigma_3^z - \sigma_4^x\sigma_5^z\sigma_6^y - \sigma_5^x\sigma_6^x. \end{aligned} \tag{35}$$

The detailed evolution of the corresponding spin state during the MZMs exchange is calculated as follows. After the ITE operation of the initial Hamiltonian

$$H_0 = -\sigma_1^x\sigma_2^x + \sigma_3^z - \sigma_4^x\sigma_5^x - \sigma_5^x\sigma_6^x, \tag{36}$$

which corresponds to creating the MZMs A, B, C and D, the state becomes

$$|\phi_0\rangle = \alpha|x_1x_2\bar{z}_3x_4x_5x_6\rangle + \beta|\bar{x}_1\bar{x}_2\bar{z}_3x_4x_5x_6\rangle + \mu|x_1x_2\bar{z}_3\bar{x}_4\bar{x}_5\bar{x}_6\rangle + \nu|\bar{x}_1\bar{x}_2\bar{z}_3\bar{x}_4\bar{x}_5\bar{x}_6\rangle, \tag{37}$$

where $\alpha$, $\beta$, $\mu$ and $\nu$ are complex amplitudes satisfying $|\alpha|^2+|\beta|^2+|\mu|^2+|\nu|^2=1$. The first step is the same as that of the braiding of A and C.

The state is then sent to the second ITE operation with Hamiltonian

$$H_1' = -\sigma_1^x\sigma_2^x + \sigma_3^z + \sigma_4^z - \sigma_5^x\sigma_6^x, \tag{38}$$

which corresponds to transporting the MZM C to site 5. We need only consider the ITE operation of $\sigma_4^z$ and the state becomes

$$|\phi_1'\rangle = \alpha|x_1x_2\bar{z}_3\bar{z}_4x_5x_6\rangle + \beta|\bar{x}_1\bar{x}_2\bar{z}_3\bar{z}_4x_5x_6\rangle - \mu|x_1x_2\bar{z}_3\bar{z}_4\bar{x}_5\bar{x}_6\rangle - \nu|\bar{x}_1\bar{x}_2\bar{z}_3\bar{z}_4\bar{x}_5\bar{x}_6\rangle. \tag{39}$$

The state $|\phi_1'\rangle$ is then sent to the ITE operation of $H_2'$

$$H_2' = -\sigma_1^x\sigma_2^x + \sigma_3^z - \sigma_4^x\sigma_5^z\sigma_6^y - \sigma_5^x\sigma_6^x, \tag{40}$$

which corresponds to transporting MZM D to site 4. For this operation only $-\sigma_4^x\sigma_5^z\sigma_6^y$ needs to be considered. The state becomes

$$\begin{aligned}|\phi_2'\rangle = \alpha((1-i)|x_1x_2\bar{z}_3x_4z_5y_6\rangle + (1+i)|x_1x_2\bar{z}_3x_4\bar{z}_5\bar{y}_6\rangle - (1+i)|x_1x_2\bar{z}_3\bar{x}_4\bar{z}_5\bar{y}_6\rangle - (1-i)|d_1d_2v_3k_4v_5l_6\rangle)\\ + \beta((1-i)|\bar{x}_1\bar{x}_2\bar{z}_3x_4z_5y_6\rangle + (1+i)|\bar{x}_1\bar{x}_2\bar{z}_3x_4\bar{z}_5\bar{y}_6\rangle - (1+i)|k_1k_2v_3k_4h_5r_6\rangle - (1-i)|k_1k_2v_3k_4v_5l_6\rangle)\\ - \mu((1+i)|x_1x_2\bar{z}_3x_4z_5y_6\rangle - (1-i)|x_1x_2\bar{z}_3x_4\bar{z}_5\bar{y}_6\rangle - (1-i)|x_1x_2\bar{z}_3\bar{x}_4z_5\bar{y}_6\rangle + (1+i)|x_1x_2\bar{z}_3\bar{x}_4\bar{z}_5y_6\rangle)\\ - \nu((1+i)|\bar{x}_1\bar{x}_2\bar{z}_3x_4z_5y_6\rangle - (1-i)|\bar{x}_1\bar{x}_2\bar{z}_3x_4\bar{z}_5\bar{y}_6\rangle - (1-i)|\bar{x}_1\bar{x}_2\bar{z}_3\bar{x}_4z_5\bar{y}_6\rangle + (1+i)|\bar{x}_1\bar{x}_2\bar{z}_3\bar{x}_4\bar{z}_5y_6\rangle).\end{aligned} \tag{41}$$

This state can be rewritten as

$$\begin{aligned}|\phi_2'\rangle = (\alpha(1-i) - \mu((1+i))|x_1x_2\bar{z}_3x_4z_5y_6\rangle + (\alpha(1+i) + \mu(1-i))|x_1x_2\bar{z}_3x_4\bar{z}_5\bar{y}_6\rangle\\ + (-\alpha(1+i) + \mu(1-i))|x_1x_2\bar{z}_3\bar{x}_4z_5\bar{y}_6\rangle + (-\alpha(1-i) - \mu(1+i))|x_1x_2\bar{z}_3\bar{x}_4\bar{z}_5y_6\rangle\\ + (\beta(1-i) - \nu(1+i))|\bar{x}_1\bar{x}_2\bar{z}_3x_4z_5y_6\rangle + (\beta(1+i) + \nu(1-i))|\bar{x}_1\bar{x}_2\bar{z}_3x_4\bar{z}_5\bar{y}_6\rangle\\ + (-\beta(1+i) + \nu(1-i))|\bar{x}_1\bar{x}_2\bar{z}_3\bar{x}_4z_5\bar{y}_6\rangle + (-\beta(1-i) - \nu(1+i))|\bar{x}_1\bar{x}_2\bar{z}_3\bar{x}_4\bar{z}_5y_6\rangle.\end{aligned} \tag{42}$$

Finally, we move back to $H_0$ which corresponds to transporting MZM C to site 6. After the ITE of $-\sigma_4^x\sigma_5^x$, the state becomes

$$\begin{aligned}|\phi_3'\rangle = (\alpha(1-i) - \mu(1+i))|x_1x_2\bar{z}_3x_4x_5y_6\rangle + (\alpha(1+i) + \mu(1-i))|x_1x_2\bar{z}_3x_4x_5\bar{y}_6\rangle\\ + (-\alpha(1+i) + \mu(1-i))|x_1x_2\bar{z}_3\bar{x}_4\bar{x}_5\bar{y}_6\rangle - (-\alpha(1-i) - \mu(1+i))|x_1x_2\bar{z}_3\bar{x}_4\bar{x}_5y_6\rangle\\ + (\beta(1-i) - \nu(1+i))|\bar{x}_1\bar{x}_2\bar{z}_3x_4x_5y_6\rangle + (\beta(1+i) + \nu(1-i))|\bar{x}_1\bar{x}_2\bar{z}_3x_4x_5\bar{y}_6\rangle\\ + (-\beta(1+i) + \nu(1-i))|\bar{x}_1\bar{x}_2\bar{z}_3\bar{x}_4\bar{x}_5\bar{y}_6\rangle - (-\beta(1-i) - \nu(1+i))|\bar{x}_1\bar{x}_2\bar{z}_3\bar{x}_4\bar{x}_5y_6\rangle.\end{aligned} \tag{43}$$

After the ITE of $-\sigma_5^x\sigma_6^x$, the state becomes

$$\begin{aligned}|\phi_3'\rangle = (\alpha - i\mu)|x_1x_2\bar{z}_3x_4x_5x_6\rangle + (\alpha - i\mu)|x_1x_2\bar{z}_3x_4x_5x_6\rangle\\ + (-i\alpha + \mu)|x_1x_2\bar{z}_3\bar{x}_4\bar{x}_5\bar{x}_6\rangle - (i\alpha - \mu)|x_1x_2\bar{z}_3\bar{x}_4\bar{x}_5\bar{x}_6\rangle\\ + (\beta - i\nu)|\bar{x}_1\bar{x}_2\bar{z}_3x_4x_5x_6\rangle + (\beta - i\nu)|\bar{x}_1\bar{x}_2\bar{z}_3x_4x_5x_6\rangle\\ + (-i\beta + \nu)|\bar{x}_1\bar{x}_2\bar{z}_3\bar{x}_4\bar{x}_5\bar{x}_6\rangle - (i\beta - \nu)|\bar{x}_1\bar{x}_2\bar{z}_3\bar{x}_4\bar{x}_5\bar{x}_6\rangle.\end{aligned} \tag{44}$$

The final state can be rewritten as

$$\begin{aligned}|\phi_3'\rangle = (\alpha - i\mu)|x_1x_2\bar{z}_3x_4x_5x_6\rangle + (-i\alpha + \mu)|x_1x_2\bar{z}_3\bar{x}_4\bar{x}_5\bar{x}_6\rangle\\ + (\beta - i\nu)|\bar{x}_1\bar{x}_2\bar{z}_3x_4x_5x_6\rangle + (-i\beta + \nu)|\bar{x}_1\bar{x}_2\bar{z}_3\bar{x}_4\bar{x}_5\bar{x}_6\rangle.\end{aligned} \tag{45}$$

To show the resulting gate operation we consider the logical basis. The transformations are given by $|x_1x_2\rangle = (|0_{12}\rangle + |1_{12}\rangle)/\sqrt{2}$, $|\bar{x}_1\bar{x}_2\rangle = (|0_{12}\rangle - |1_{12}\rangle)/\sqrt{2}$, $|x_4x_5x_6\rangle = (|0_{456}\rangle + |1_{456}\rangle)/\sqrt{2}$ and $|\bar{x}_4\bar{x}_5\bar{x}_6\rangle = (|1_{456}\rangle - |0_{456}\rangle)/\sqrt{2}$ (see Methods part). As a result, $|0_{12}0_{456}\rangle|\bar{z}_3\rangle = |00_g\rangle$, $|0_{12}1_{456}\rangle|\bar{z}_3\rangle = |01_g\rangle$, $|1_{12}0_{456}\rangle|\bar{z}_3\rangle = |10_g\rangle$ and $|1_{12}1_{456}\rangle|\bar{z}_3\rangle = |11_g\rangle$.

The initial state (ground state of $H_0$) can be written as

$$\begin{aligned}|\phi_0\rangle &= \alpha|x_1x_2\bar{z}_3x_4x_5x_6\rangle + \beta|\bar{x}_1\bar{x}_2\bar{z}_3x_4x_5x_6\rangle + \mu|x_1x_2\bar{z}_3\bar{x}_4\bar{x}_5\bar{x}_6\rangle + \nu|\bar{x}_1\bar{x}_2\bar{z}_3\bar{x}_4\bar{x}_5\bar{x}_6\rangle \\ &= (\alpha+\beta-\mu-\nu)|00_g\rangle + (\alpha+\beta+\mu+\nu)|01_g\rangle \\ &\quad + (\alpha-\beta-\mu+\nu)|10_g\rangle + (\alpha-\beta+\mu-\nu)|11_g\rangle.\end{aligned} \tag{46}$$

After the exchange process, the final state becomes in the logic basis

$$\begin{aligned}|\phi_3'\rangle &= (\alpha - i\mu)|x_1x_2\bar{z}_3x_4x_5x_6\rangle + (-i\alpha+\mu)|x_1x_2\bar{z}_3\bar{x}_4\bar{x}_5\bar{x}_6\rangle \\ &\quad + (\beta - i\nu)|\bar{x}_1\bar{x}_2\bar{z}_3x_4x_5x_6\rangle + (-i\beta+\nu)|\bar{x}_1\bar{x}_2\bar{z}_3\bar{x}_4\bar{x}_5\bar{x}_6\rangle. \\ &= i(\alpha+\beta-\mu-\nu)|00_g\rangle + (\alpha+\beta+\mu+\nu)|01_g\rangle \\ &\quad + i(\alpha-\beta-\mu+\nu)|10_g\rangle + (\alpha-\beta+\mu-\nu)|11_g\rangle\end{aligned} \tag{47}$$

As a result, the unitary transformation of the anticlockwise braiding of MZMs C and D reads as

$$U = \begin{pmatrix} 1 & 0 & 0 & 0 \\ 0 & -i & 0 & 0 \\ 0 & 0 & 1 & 0 \\ 0 & 0 & 0 & -i \end{pmatrix}, \tag{48}$$

given in the basis $\{|00_g\rangle, |01_g\rangle, |10_g\rangle, |11_g\rangle\}$. If we focus on the even fermionic parity space spanned by $|00_g\rangle$ and $|11_g\rangle$, the unitary transformation becomes

$$U = \begin{pmatrix} 1 & 0 \\ 0 & -i \end{pmatrix}. \tag{49}$$

A similar calculation can be performed to determine the evolution of the clockwise braiding of the MZMs C and D, as shown in Fig. S5.

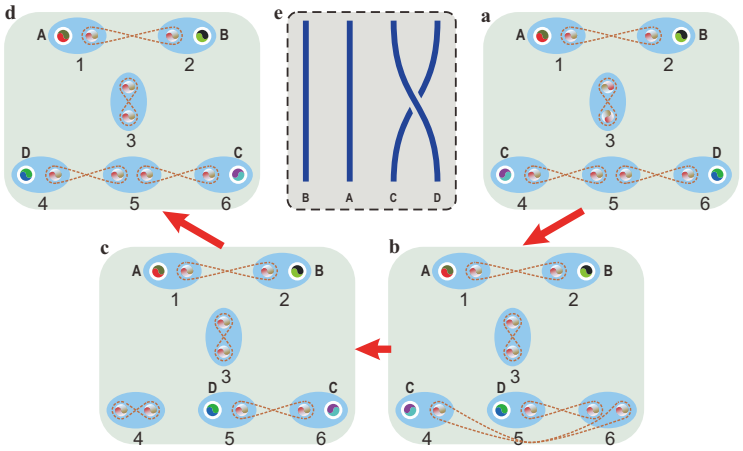


Fig. S5. The process of clockwise braiding of MZMs C and D. The Kitaev chains consist of six fermions (numbered from 1 to 6) with four isolated endpoint MZMs A, B, C and D. Each two particles in the blue ellipse form a conventional fermion. The dashed lines between different Majorana fermions ($k$ and $l$= $1a, 1b, \cdots, 6b$) represent the interactions, $i\gamma_k\gamma_l$, between them. **a**, **b**, **c**, **d** correspond to the imaginary-time evolution of Hamiltonians similar to the clockwise braiding of the MZMs C and D. **e.** The worldline strands representing the clockwise braiding of the C and D MZMs.

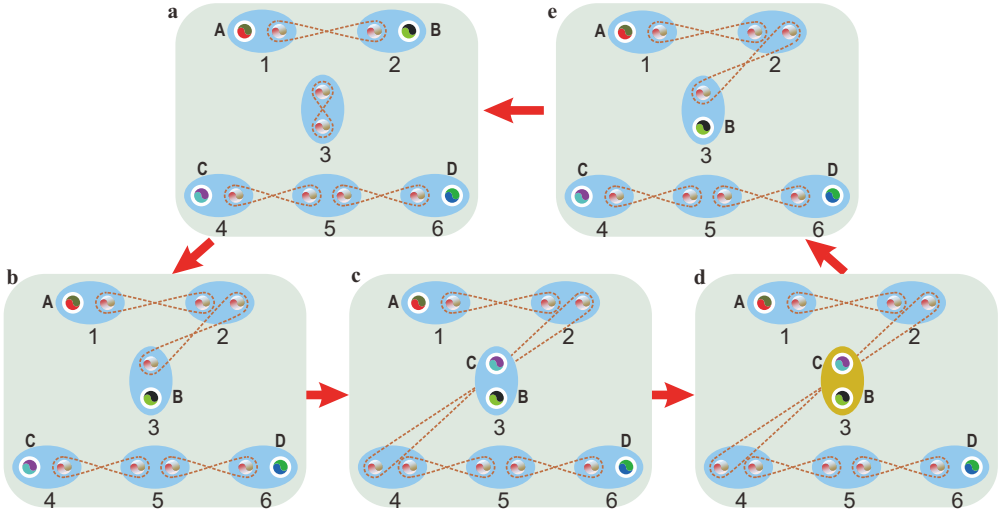


Fig. S6. The process for implementing the phase gate based on the dynamics of MZMs. The Kitaev chains consist of six fermions (numbered from 1 to 6) with four isolated endpoint MZMs A, B, C and D. Each two particles in the blue ellipse form a conventional fermion. The dashed lines between different Majorana fermions ($k$ and $l$ = $1a, 1b, \cdots, 6b$) represent the interactions, $i\gamma_k\gamma_l$, between them. **a**, **b**, **c** and **e** correspond to the imaginary-time evolution of the Hamiltonian $H_0$, $H_1''$, $H_2''$ and $H_3''$, respectively. The real time evolution of $H_e''$ is implemented on **d**, where MZMs B and C are on the same site (site 3).

### D. The state evolution during the $\frac{\pi}{8}$-phase gate

The process that implements the $\frac{\pi}{8}$-phase gate, which is not topologically protected, is described in Fig. S6. This gate is implemented by the following fermionic Hamiltonians

$$\begin{aligned}
H_{M_0} &= i(\gamma_{1b}\gamma_{2a} + \gamma_{4b}\gamma_{5a} + \gamma_{5b}\gamma_{6a}) + i\gamma_{3a}\gamma_{3b}, \\
H_{p_1} &= i(\gamma_{1b}\gamma_{2a} + \gamma_{2b}\gamma_{3a} + \gamma_{4b}\gamma_{5a} + \gamma_{5b}\gamma_{6a}), \\
H_{p_2} &= i(\gamma_{1b}\gamma_{2a} + \gamma_{2b}\gamma_{4a} + \gamma_{4b}\gamma_{5a} + \gamma_{5b}\gamma_{6a}), \\
H_e &= -i\gamma_{3a}\gamma_{3b}, \\
H_{p_1} &= i(\gamma_{1b}\gamma_{2a} + \gamma_{2b}\gamma_{3a} + \gamma_{4b}\gamma_{5a} + \gamma_{5b}\gamma_{6a}).
\end{aligned} \tag{50}$$

The adiabatic evolution for the implementation of this gate can be simulated in terms of spins. The corresponding Hamiltonians are given by

$$\begin{aligned}
H_0 &= -\sigma_1^x\sigma_2^x + \sigma_3^z - \sigma_4^x\sigma_5^x - \sigma_5^x\sigma_6^x, \\
H_1'' &= -\sigma_1^x\sigma_2^x - \sigma_2^x\sigma_3^x - \sigma_4^x\sigma_5^x - \sigma_5^x\sigma_6^x, \\
H_2'' &= -\sigma_1^x\sigma_2^x + \sigma_2^x\sigma_3^z\sigma_4^x - \sigma_4^x\sigma_5^x - \sigma_5^x\sigma_6^x, \\
H_e'' &= -\sigma_3^z, \\
H_1'' &= -\sigma_1^x\sigma_2^x - \sigma_2^x\sigma_3^x - \sigma_4^x\sigma_5^x - \sigma_5^x\sigma_6^x.
\end{aligned} \tag{51}$$

The evolution of the ground state during the adiabatic transitions is calculated as follows. After the ITE operation of the initial Hamiltonian

$$H_0 = -\sigma_1^x\sigma_2^x + \sigma_3^z - \sigma_4^x\sigma_5^x - \sigma_5^x\sigma_6^x, \tag{52}$$

which corresponds to creating the MZMs A, B, C and D, the state becomes

$$|\phi_0\rangle = \alpha|x_1x_2\bar{z}_3x_4x_5x_6\rangle + \beta|\bar{x}_1\bar{x}_2\bar{z}_3x_4x_5x_6\rangle + \mu|x_1x_2\bar{z}_3\bar{x}_4\bar{x}_5\bar{x}_6\rangle + \nu|\bar{x}_1\bar{x}_2\bar{z}_3\bar{x}_4\bar{x}_5\bar{x}_6\rangle, \tag{53}$$

where $\alpha$, $\beta$, $\mu$ and $\nu$ are complex amplitudes satisfying $|\alpha|^2 + |\beta|^2 + |\mu|^2 + |\nu|^2 = 1$. The first step is the same as that from braiding the MZMs A and C. The state is then sent to the second ITE operation with the Hamiltonian

$$H_1'' = -\sigma_1^x\sigma_2^x - \sigma_2^x\sigma_3^x - \sigma_4^x\sigma_5^x - \sigma_5^x\sigma_6^x, \tag{54}$$

which corresponds to transporting MZM B to site 3. To perform this step we only need to consider the ITE operation of $-\sigma_2^x\sigma_3^x$ and the state becomes

$$\begin{aligned}|\phi_1''\rangle &= \alpha|x_1x_2\bar{z}_3x_4x_5x_6\rangle + \beta|\bar{x}_1\bar{x}_2\bar{z}_3x_4x_5x_6\rangle + \mu|x_1x_2\bar{z}_3\bar{x}_4\bar{x}_5\bar{x}_6\rangle + \nu|\bar{x}_1\bar{x}_2\bar{z}_3\bar{x}_4\bar{x}_5\bar{x}_6\rangle \\ &= \alpha|x_1x_2(x_3-\bar{x}_3)x_4x_5x_6\rangle + \beta|\bar{x}_1\bar{x}_2(x_3-\bar{x}_3)x_4x_5x_6\rangle \\ &\quad + \mu|x_1x_2(x_3-\bar{x}_3)\bar{x}_4\bar{x}_5\bar{x}_6\rangle + \nu|\bar{x}_1\bar{x}_2(x_3-\bar{x}_3)\bar{x}_4\bar{x}_5\bar{x}_6\rangle \\ &= \alpha|x_1x_2x_3x_4x_5x_6\rangle - \beta|\bar{x}_1\bar{x}_2\bar{x}_3x_4x_5x_6\rangle + \mu|x_1x_2x_3\bar{x}_4\bar{x}_5\bar{x}_6\rangle - \nu|\bar{x}_1\bar{x}_2\bar{x}_3\bar{x}_4\bar{x}_5\bar{x}_6\rangle.\end{aligned} \tag{55}$$

The state $|\phi_1''\rangle$ is then sent to the ITE operation of

$$H_2'' = -\sigma_1^x\sigma_2^x + \sigma_2^x\sigma_3^z\sigma_4^x - \sigma_4^x\sigma_5^x - \sigma_5^x\sigma_6^x, \tag{56}$$

which corresponds to transporting MZM C to the same site 3. Only the term of $\sigma_2^x\sigma_3^z\sigma_4^x$ needs to be implemented. The state then becomes

$$\begin{aligned}|\phi_2''\rangle &= \alpha|x_1x_2x_3x_4x_5x_6\rangle - \beta|\bar{x}_1\bar{x}_2\bar{x}_3x_4x_5x_6\rangle + \mu|x_1x_2x_3\bar{x}_4\bar{x}_5\bar{x}_6\rangle - \nu|\bar{x}_1\bar{x}_2\bar{x}_3\bar{x}_4\bar{x}_5\bar{x}_6\rangle \\ &= \alpha|x_1x_2(z_3+\bar{z}_3)x_4x_5x_6\rangle - \beta|\bar{x}_1\bar{x}_2(z_3-\bar{z}_3)x_4x_5x_6\rangle \\ &\quad + \mu|x_1x_2(z_3+\bar{z}_3)\bar{x}_4\bar{x}_5\bar{x}_6\rangle - \nu|\bar{x}_1\bar{x}_2(z_3-\bar{z}_3)\bar{x}_4\bar{x}_5\bar{x}_6\rangle \\ &= \alpha|x_1x_2\bar{z}_3x_4x_5x_6\rangle - \beta|\bar{x}_1\bar{x}_2z_3x_4x_5x_6\rangle + \mu|x_1x_2z_3\bar{x}_4\bar{x}_5\bar{x}_6\rangle + \nu|\bar{x}_1\bar{x}_2\bar{z}_3\bar{x}_4\bar{x}_5\bar{x}_6\rangle.\end{aligned} \tag{57}$$

We then implement the real time evolution of $H_e''$ on site 3 with the evolution operation $e^{i\sigma_3^z\tau}$, where $\tau$ is the corresponding evolution time, resulting to

$$|\phi_2''\rangle^\tau = e^{-i\tau}\alpha|x_1x_2\bar{z}_3x_4x_5x_6\rangle - e^{i\tau}\beta|\bar{x}_1\bar{x}_2z_3x_4x_5x_6\rangle + e^{i\tau}\mu|x_1x_2z_3\bar{x}_4\bar{x}_5\bar{x}_6\rangle + e^{-i\tau}\nu|\bar{x}_1\bar{x}_2\bar{z}_3\bar{x}_4\bar{x}_5\bar{x}_6\rangle. \tag{58}$$

The state then further passes through ITE of the the Hamiltonian

$$H_1'' = -\sigma_1^x\sigma_2^x - \sigma_2^x\sigma_3^x - \sigma_4^x\sigma_5^x - \sigma_5^x\sigma_6^x, \tag{59}$$

which corresponds to transporting MZM C back to site 4. From this Hamiltonian we only need to consider the term of $-\sigma_2^x\sigma_3^x$ for the application of the ITE. The state then becomes

$$\begin{aligned}|\phi_3''\rangle &= e^{-i\tau}\alpha|x_1x_2\bar{z}_3x_4x_5x_6\rangle - e^{i\tau}\beta|\bar{x}_1\bar{x}_2z_3x_4x_5x_6\rangle + e^{i\tau}\mu|x_1x_2z_3\bar{x}_4\bar{x}_5\bar{x}_6\rangle + e^{-i\tau}\nu|\bar{x}_1\bar{x}_2\bar{z}_3\bar{x}_4\bar{x}_5\bar{x}_6\rangle \\ &= e^{-i\tau}\alpha|x_1x_2(x_3-\bar{x}_3)x_4x_5x_6\rangle - e^{i\tau}\beta|\bar{x}_1\bar{x}_2(x_3+\bar{x}_3)x_4x_5x_6\rangle \\ &\quad + e^{i\tau}\mu|x_1x_2(x_3+\bar{x}_3)\bar{x}_4\bar{x}_5\bar{x}_6\rangle + e^{-i\tau}\nu|\bar{x}_1\bar{x}_2(x_3-\bar{x}_3)\bar{x}_4\bar{x}_5\bar{x}_6\rangle \\ &= e^{-i\tau}\alpha|x_1x_2x_3x_4x_5x_6\rangle - e^{i\tau}\beta|\bar{x}_1\bar{x}_2\bar{x}_3x_4x_5x_6\rangle \\ &\quad + e^{i\tau}\mu|x_1x_2x_3\bar{x}_4\bar{x}_5\bar{x}_6\rangle - e^{-i\tau}\nu|\bar{x}_1\bar{x}_2\bar{x}_3\bar{x}_4\bar{x}_5\bar{x}_6\rangle.\end{aligned} \tag{60}$$

Finally, we project the state back to the ground state space of the initial Hamiltonian

$$H_0 = -\sigma_1^x\sigma_2^x + \sigma_3^z - \sigma_4^x\sigma_5^x - \sigma_5^x\sigma_6^x, \tag{61}$$

which corresponds to transporting MZM B back to site 2. The state becomes

$$\begin{aligned}
|\phi_4''\rangle &= e^{-i\tau}\alpha|x_1x_2x_3x_4x_5x_6\rangle - e^{i\tau}\beta|\bar{x}_1\bar{x}_2\bar{x}_3x_4x_5x_6\rangle \\
&\quad + e^{i\tau}\mu|x_1x_2x_3\bar{x}_4\bar{x}_5\bar{x}_6\rangle - e^{-i\tau}\nu|\bar{x}_1\bar{x}_2\bar{x}_3\bar{x}_4\bar{x}_5\bar{x}_6\rangle \\
&= e^{-i\tau}\alpha|x_1x_2(z_3+\bar{z}_3)x_4x_5x_6\rangle - e^{i\tau}\beta|\bar{x}_1\bar{x}_2(z_3-\bar{z}_3)x_4x_5x_6\rangle \\
&\quad + e^{i\tau}\mu|x_1x_2(z_3+\bar{z}_3)\bar{x}_4\bar{x}_5\bar{x}_6\rangle - e^{-i\tau}\nu|\bar{x}_1\bar{x}_2(z_3-\bar{z}_3)\bar{x}_4\bar{x}_5\bar{x}_6\rangle \\
&= e^{-i\tau}\alpha|x_1x_2\bar{z}_3x_4x_5x_6\rangle + e^{i\tau}\beta|\bar{x}_1\bar{x}_2\bar{z}_3x_4x_5x_6\rangle + e^{i\tau}\mu|x_1x_2\bar{z}_3\bar{x}_4\bar{x}_5\bar{x}_6\rangle + e^{-i\tau}\nu|\bar{x}_1\bar{x}_2\bar{z}_3\bar{x}_4\bar{x}_5\bar{x}_6\rangle
\end{aligned} \tag{62}$$

To determine the effect of these evolutions on the logical space, we translate the basis by $|x_1x_2\rangle = (|0_{12}\rangle + |1_{12}\rangle)/\sqrt{2}$, $|\bar{x}_1\bar{x}_2\rangle = (|0_{12}\rangle - |1_{12}\rangle)/\sqrt{2}$, $|x_4x_5x_6\rangle = (|0_{456}\rangle + |1_{456}\rangle)/\sqrt{2}$ and $|\bar{x}_4\bar{x}_5\bar{x}_6\rangle = (|1_{456}\rangle - |0_{456}\rangle)/\sqrt{2}$. The logical basis is then defined as $|0_{12}0_{456}\rangle|\bar{z}_3\rangle = |00_g\rangle$, $|0_{12}1_{456}\rangle|\bar{z}_3\rangle = |01_g\rangle$, $|1_{12}0_{456}\rangle|\bar{z}_3\rangle = |10_g\rangle$ and $|1_{12}1_{456}\rangle|\bar{z}_3\rangle = |11_g\rangle$.

The initial state (ground state of $H_0$) becomes

$$\begin{aligned}
|\phi_0\rangle &= \alpha|x_1x_2\bar{z}_3x_4x_5x_6\rangle + \beta|\bar{x}_1\bar{x}_2\bar{z}_3x_4x_5x_6\rangle + \mu|x_1x_2\bar{z}_3\bar{x}_4\bar{x}_5\bar{x}_6\rangle + \nu|\bar{x}_1\bar{x}_2\bar{z}_3\bar{x}_4\bar{x}_5\bar{x}_6\rangle \\
&= (\alpha+\beta-\mu-\nu)|00_g\rangle + (\alpha+\beta+\mu+\nu)|01_g\rangle \\
&\quad + (\alpha-\beta-\mu+\nu)|10_g\rangle + (\alpha-\beta+\mu-\nu)|11_g\rangle.
\end{aligned} \tag{63}$$

After the phase gate operation the final state becomes

$$\begin{aligned}
|\phi_4'\rangle &= (e^{-i\tau}\alpha + e^{i\tau}\beta - e^{i\tau}\mu - e^{-i\tau}\nu)|0_{12}0_{456}\rangle|v_3\rangle + (e^{-i\tau}\alpha + e^{i\tau}\beta + e^{i\tau}\mu + e^{-i\tau}\nu)|0_{12}1_{456}\rangle|v_3\rangle \\
&\quad + (e^{-i\tau}\alpha - e^{i\tau}\beta - e^{i\tau}\mu + e^{-i\tau}\nu)|1_{12}0_{456}\rangle|v_3\rangle + (e^{-i\tau}\alpha - e^{i\tau}\beta + e^{i\tau}\mu - e^{i\tau}\nu)|1_{12}1_{456}\rangle|v_3\rangle \\
&= [(\alpha+\beta-\mu-\nu)\cos\tau - (\alpha-\beta+\mu-\nu)i\sin\tau]|00_g\rangle \\
&\quad + [(\alpha+\beta+\mu+\nu)\cos\tau - (\alpha-\beta-\mu+\nu)i\sin\tau]|01_g\rangle \\
&\quad + [(\alpha-\beta-\mu+\nu)\cos\tau - (\alpha+\beta+\mu+\nu)i\sin\tau]|10_g\rangle \\
&\quad + [(\alpha-\beta+\mu-\nu)\cos\tau - (\alpha+\beta-\mu-\nu)i\sin\tau]|10_g\rangle.
\end{aligned} \tag{64}$$

Compared to the initial state, the operation is written as

$$U = \begin{pmatrix} \cos\tau & 0 & 0 & -i\sin\tau \\ 0 & \cos\tau & -i\sin\tau & 0 \\ 0 & -i\sin\tau & \cos\tau & 0 \\ -i\sin\tau & 0 & 0 & \cos\tau \end{pmatrix}, \tag{65}$$

expressed in the basis $\{|00_g\rangle, |01_g\rangle, |10_g\rangle, |11_g\rangle\}$.

If we focus on the even fermionic parity basis of $|00_g\rangle$ and $|11_g\rangle$, the phase operation becomes

$$U = \begin{pmatrix} \cos\tau & -i\sin\tau \\ -i\sin\tau & \cos\tau \end{pmatrix}. \tag{66}$$

With the help of the Hadamard gate $H$ we can obtain the phase gate as $H^\dagger M H = e^{-i\tau}\begin{pmatrix} 1 & 0 \\ 0 & e^{2i\tau} \end{pmatrix}$. Thus, the $\frac{\pi}{8}$-phase gate can be achieved by controlling the time to be $\tau = \frac{\pi}{8}$.

### E. Effect of the phase errors on site 4 during the phase gate

As discussed in [31], phase errors, caused by $c_j^\dagger c_j$, are dominant in fermionic system. Generally, the error operator can be written as $e^{-ic_j^\dagger c_j t}$ where $t$ is the interaction time. We can expand the operator as

$$e^{ic^\dagger c\, t} = \sum_{n=0}^{\infty} \frac{(ic^\dagger c\, t)^n}{n!} = 1 + (e^{-it} - 1)c^\dagger c. \tag{67}$$

Hence, to demonstrate the influence of the phase error, we only need to consider the action of the operator $c^\dagger c$ (which is transformed to $(1+\sigma^z)/2$ in the spin representation) in the ground-state space. We first consider the action of the noise on site 4. In this case, at most one MZM is effected, so we expect the information encoded in the MZMs to be robust. To demonstrate this characteristic, we assume that the error happens during the phase gate operation.

The evolution of the state during the phase gate with the presence of the phase error is determined as follows. After the ITE operation of the initial Hamiltonian

$$H_0 = -\sigma_1^x\sigma_2^x + \sigma_3^z - \sigma_4^x\sigma_5^x - \sigma_5^x\sigma_6^x, \tag{68}$$

the state becomes

$$|\phi_0\rangle = \alpha|x_1x_2\bar{z}_3x_4x_5x_6\rangle + \beta|\bar{x}_1\bar{x}_2\bar{z}_3x_4x_5x_6\rangle + \mu|x_1x_2\bar{z}_3\bar{x}_4\bar{x}_5\bar{x}_6\rangle + \nu|\bar{x}_1\bar{x}_2\bar{z}_3\bar{x}_4\bar{x}_5\bar{x}_6\rangle. \quad (69)$$

The phase error operation is then implemented and the state becomes

$$\begin{aligned}|\phi_0\rangle_{err} = 1/2(\alpha|x_1x_2\bar{z}_3x_4x_5x_6\rangle + \beta|\bar{x}_1\bar{x}_2\bar{z}_3x_4x_5x_6\rangle + \mu|x_1x_2\bar{z}_3\bar{x}_4\bar{x}_5\bar{x}_6\rangle + \nu|\bar{x}_1\bar{x}_2\bar{z}_3\bar{x}_4\bar{x}_5\bar{x}_6\rangle)\\ + 1/2(\alpha|x_1x_2\bar{z}_3\bar{x}_4x_5x_6\rangle + \beta|\bar{x}_1\bar{x}_2\bar{z}_3\bar{x}_4x_5x_6\rangle + \mu|x_1x_2\bar{z}_3x_4\bar{x}_5\bar{x}_6\rangle + \nu|x_1x_2\bar{z}_3x_4\bar{x}_5\bar{x}_6\rangle).\end{aligned} \quad (70)$$

There is a probability of 0.5 that the state of particle 4 changes from $x_4$ to $\bar{x}_4$. The state is then transformed by the second ITE operation with the Hamiltonian

$$H_1'' = -\sigma_1^x\sigma_2^x - \sigma_2^x\sigma_3^x - \sigma_4^x\sigma_5^x - \sigma_5^x\sigma_6^x. \quad (71)$$

The terms disturbed by the operation $\sigma_4^z$ is discarded due to the ITE operation of the similar Hamiltonian $-\sigma_4^x\sigma_5^x$ and the state becomes

$$|\phi_1''\rangle = \alpha|x_1x_2x_3x_4x_5x_6\rangle - \beta|\bar{x}_1\bar{x}_2\bar{x}_3x_4x_5x_6\rangle + \mu|x_1x_2x_3\bar{x}_4\bar{x}_5\bar{x}_6\rangle - \nu|\bar{x}_1\bar{x}_2\bar{x}_3\bar{x}_4\bar{x}_5\bar{x}_6\rangle. \quad (72)$$

The phase error operation is then implemented and the state becomes

$$\begin{aligned}|\phi_1''\rangle_{err} = 1/2(\alpha|x_1x_2x_3x_4x_5x_6\rangle - \beta|\bar{x}_1\bar{x}_2\bar{x}_3x_4x_5x_6\rangle + \mu|x_1x_2x_3\bar{x}_4\bar{x}_5\bar{x}_6\rangle - \nu|\bar{x}_1\bar{x}_2\bar{x}_3\bar{x}_4\bar{x}_5\bar{x}_6\rangle)\\ + 1/2(\alpha|x_1x_2x_3\bar{x}_4x_5x_6\rangle - \beta|\bar{x}_1\bar{x}_2\bar{x}_3\bar{x}_4x_5x_6\rangle + \mu|x_1x_2x_3x_4\bar{x}_5\bar{x}_6\rangle - \nu|x_1x_2\bar{x}_3x_4\bar{x}_5\bar{x}_6\rangle).\end{aligned} \quad (73)$$

The next ITE operation is with respect to

$$H_2'' = -\sigma_1^x\sigma_2^x + \sigma_2^x\sigma_3^z\sigma_4^x - \sigma_4^x\sigma_5^x - \sigma_5^x\sigma_6^x, \quad (74)$$

and the state becomes

$$|\phi_2''\rangle = \alpha|x_1x_2\bar{z}_3x_4x_5x_6\rangle - \beta|\bar{x}_1\bar{x}_2z_3x_4x_5x_6\rangle + \mu|x_1x_2z_3\bar{x}_4\bar{x}_5\bar{x}_6\rangle + \nu|\bar{x}_1\bar{x}_2\bar{z}_3\bar{x}_4\bar{x}_5\bar{x}_6\rangle. \quad (75)$$

The phase error operation is again implemented and the state becomes

$$\begin{aligned}|\phi_2''\rangle_{err} = 1/2(\alpha|x_1x_2\bar{z}_3x_4x_5x_6\rangle - \beta|\bar{x}_1\bar{x}_2z_3x_4x_5x_6\rangle + \mu|x_1x_2z_3\bar{x}_4\bar{x}_5\bar{x}_6\rangle + \nu|\bar{x}_1\bar{x}_2\bar{z}_3\bar{x}_4\bar{x}_5\bar{x}_6\rangle)\\ + 1/2(\alpha|x_1x_2\bar{z}_3\bar{x}_4x_5x_6\rangle - \beta|\bar{x}_1\bar{x}_2z_3\bar{x}_4x_5x_6\rangle + \mu|x_1x_2z_3x_4\bar{x}_5\bar{x}_6\rangle + \nu|\bar{x}_1\bar{x}_2\bar{z}_3x_4\bar{x}_5\bar{x}_6\rangle).\end{aligned} \quad (76)$$

By implementing the real time evolution of $e^{i\sigma_3^z}$ on site 3 with the time $\tau$, the state becomes

$$|\phi_2''\rangle_{err}^{\tau} = 1/2(e^{-i\tau}\alpha|x_1x_2\bar{z}_3x_4x_5x_6\rangle - e^{i\tau}\beta|\bar{x}_1\bar{x}_2z_3x_4x_5x_6\rangle + e^{i\tau}\mu|x_1x_2z_3\bar{x}_4\bar{x}_5\bar{x}_6\rangle + e^{-i\tau}\nu|\bar{x}_1\bar{x}_2\bar{z}_3\bar{x}_4\bar{x}_5\bar{x}_6\rangle)$$
$$+ 1/2(e^{-i\tau}\alpha|x_1x_2\bar{z}_3\bar{x}_4x_5x_6\rangle - e^{i\tau}\beta|\bar{x}_1\bar{x}_2z_3\bar{x}_4x_5x_6\rangle + e^{i\tau}\mu|x_1x_2z_3x_4\bar{x}_5\bar{x}_6\rangle + e^{-i\tau}\nu|\bar{x}_1\bar{x}_2\bar{z}_3x_4\bar{x}_5\bar{x}_6\rangle). \tag{77}$$

The state is then further transformed by the ITE of Hamiltonian

$$H_3'' = -\sigma_1^x\sigma_2^x - \sigma_2^x\sigma_3^x - \sigma_4^x\sigma_5^x - \sigma_5^x\sigma_6^x, \tag{78}$$

and becomes

$$|\phi_3''\rangle = e^{-i\tau}\alpha|x_1x_2x_3x_4x_5x_6\rangle - e^{i\tau}\beta|\bar{x}_1\bar{x}_2\bar{x}_3x_4x_5x_6\rangle + e^{i\tau}\mu|x_1x_2x_3\bar{x}_4\bar{x}_5\bar{x}_6\rangle - e^{-i\tau}\nu|\bar{x}_1\bar{x}_2\bar{x}_3\bar{x}_4\bar{x}_5\bar{x}_6\rangle. \tag{79}$$

The phase error operation is subsequently implemented and the state becomes

$$|\phi_3''\rangle_{err} = 1/2(e^{-i\tau}\alpha|x_1x_2x_3x_4x_5x_6\rangle - e^{i\tau}\beta|\bar{x}_1\bar{x}_2\bar{x}_3x_4x_5x_6\rangle + e^{i\tau}\mu|x_1x_2x_3\bar{x}_4\bar{x}_5\bar{x}_6\rangle - e^{-i\tau}\nu|\bar{x}_1\bar{x}_2\bar{x}_3\bar{x}_4\bar{x}_5\bar{x}_6\rangle)$$
$$+ 1/2(e^{-i\tau}\alpha|x_1x_2x_3\bar{x}_4x_5x_6\rangle - e^{i\tau}\beta|\bar{x}_1\bar{x}_2\bar{x}_3\bar{x}_4x_5x_6\rangle + e^{i\tau}\mu|x_1x_2x_3x_4\bar{x}_5\bar{x}_6\rangle - e^{-i\tau}\nu|\bar{x}_1\bar{x}_2\bar{x}_3x_4\bar{x}_5\bar{x}_6\rangle). \tag{80}$$

Finally, the state is projected back to the ground-state space of the initial Hamiltonian

$$H_0 = -\sigma_1^x\sigma_2^x + \sigma_3^z - \sigma_4^x\sigma_5^x - \sigma_5^x\sigma_6^x, \tag{81}$$

and the state becomes

$$\begin{aligned}|\phi_4''\rangle &= e^{-i\tau}\alpha|x_1x_2\bar{z}_3x_4x_5x_6\rangle + e^{i\tau}\beta|\bar{x}_1\bar{x}_2\bar{z}_3x_4x_5x_6\rangle + e^{i\tau}\mu|x_1x_2\bar{z}_3\bar{x}_4\bar{x}_5\bar{x}_6\rangle + e^{-i\tau}\nu|\bar{x}_1\bar{x}_2\bar{z}_3\bar{x}_4\bar{x}_5\bar{x}_6\rangle,\\
&= (e^{-i\tau}\alpha + e^{i\tau}\beta - e^{i\tau}\mu - e^{-i\tau}\nu)|0_{12}0_{456}\rangle|v_3\rangle + (e^{-i\tau}\alpha + e^{i\tau}\beta + e^{i\tau}\mu + e^{-i\tau}\nu)|0_{12}1_{456}\rangle|v_3\rangle\\
&+ (e^{-i\tau}\alpha - e^{i\tau}\beta - e^{i\tau}\mu + e^{i\tau}\nu)|1_{12}0_{456}\rangle|v_3\rangle + (e^{-i\tau}\alpha - e^{i\tau}\beta + e^{i\tau}\mu - e^{-i\tau}\nu)|1_{12}1_{456}\rangle|v_3\rangle\\
&= (e^{-i\tau}\alpha + e^{i\tau}\beta - e^{i\tau}\mu - e^{-i\tau}\nu)|00_g\rangle + (e^{-i\tau}\alpha + e^{i\tau}\beta + e^{i\tau}\mu + e^{-i\tau}\nu)|01_g\rangle\\
&+ (e^{-i\tau}\alpha - e^{i\tau}\beta - e^{i\tau}\mu + e^{i\tau}\nu)|10_g\rangle + (e^{-i\tau}\alpha - e^{i\tau}\beta + e^{i\tau}\mu - e^{-i\tau}\nu)|11_g\rangle,\end{aligned} \tag{82}$$

which is the same as that without error.

### F. Effect of the phase errors on site 3 during the phase gate

We now consider the effect of the phase error on site 3. Since two MZMs will simultaneously appear on this site, the phase error, given by the operator $c^\dagger c$, will induce error in the logical state during the implementation of the $\frac{\pi}{8}$-phase gate. To demonstrate exactly the effect of the error, we suppose it only operates on site 3 when two MZMs are both transported there. The state evolution during the phase gate with the error is calculated as follows.

After the ITE operation of the initial Hamiltonian

$$H_0 = -\sigma_1^x\sigma_2^x + \sigma_3^z - \sigma_4^x\sigma_5^x - \sigma_5^x\sigma_6^x, \tag{83}$$

the state becomes

$$|\phi_0\rangle = \alpha|x_1x_2\bar{z}_3x_4x_5x_6\rangle + \beta|\bar{x}_1\bar{x}_2\bar{z}_3x_4x_5x_6\rangle + \mu|x_1x_2\bar{z}_3\bar{x}_4\bar{x}_5\bar{x}_6\rangle + \nu|\bar{x}_1\bar{x}_2\bar{z}_3\bar{x}_4\bar{x}_5\bar{x}_6\rangle. \tag{84}$$

The state is then sent to the second ITE operation corresponding to the Hamiltonian

$$H_1'' = -\sigma_1^x\sigma_2^x - \sigma_2^x\sigma_3^x - \sigma_4^x\sigma_5^x - \sigma_5^x\sigma_6^x, \tag{85}$$

and the state becomes

$$|\phi_1''\rangle = \alpha|x_1x_2x_3x_4x_5x_6\rangle - \beta|\bar{x}_1\bar{x}_2\bar{x}_3x_4x_5x_6\rangle + \mu|x_1x_2x_3\bar{x}_4\bar{x}_5\bar{x}_6\rangle - \nu|\bar{x}_1\bar{x}_2\bar{x}_3\bar{x}_4\bar{x}_5\bar{x}_6\rangle. \tag{86}$$

The next ITE operation is with respect to $H_2''$

$$H_2'' = -\sigma_1^x\sigma_2^x + \sigma_2^x\sigma_3^z\sigma_4^x - \sigma_4^x\sigma_5^x - \sigma_5^x\sigma_6^x, \tag{87}$$

and the state becomes

$$|\phi_2''\rangle = \alpha|x_1x_2\bar{z}_3x_4x_5x_6\rangle - \beta|\bar{x}_1\bar{x}_2z_3x_4x_5x_6\rangle + \mu|x_1x_2z_3\bar{x}_4\bar{x}_5\bar{x}_6\rangle + \nu|\bar{x}_1\bar{x}_2\bar{z}_3\bar{x}_4\bar{x}_5\bar{x}_6\rangle. \tag{88}$$

The phase error operation is then implemented and the state becomes

$$\begin{aligned}|\phi_2''\rangle_{err} &= (\alpha|x_1x_2\bar{z}_3x_4x_5x_6\rangle - \beta|\bar{x}_1\bar{x}_2z_3x_4x_5x_6\rangle + \mu|x_1x_2z_3\bar{x}_4\bar{x}_5\bar{x}_6\rangle + \nu|\bar{x}_1\bar{x}_2\bar{z}_3\bar{x}_4\bar{x}_5\bar{x}_6\rangle)/2 \\ &+ (-\alpha|x_1x_2\bar{z}_3x_4x_5x_6\rangle - \beta|\bar{x}_1\bar{x}_2z_3x_4x_5x_6\rangle + \mu|x_1x_2z_3\bar{x}_4\bar{x}_5\bar{x}_6\rangle - \nu|\bar{x}_1\bar{x}_2\bar{z}_3\bar{x}_4\bar{x}_5\bar{x}_6\rangle)/2 \\ &= \beta|\bar{x}_1\bar{x}_2z_3x_4x_5x_6\rangle - \mu|x_1x_2z_3\bar{x}_4\bar{x}_5\bar{x}_6\rangle.\end{aligned} \tag{89}$$

There are interferences between the disturbed (the operation of $\sigma_3^z$) and undisturbed terms. By implementing the real time evolution of $e^{i\sigma_3^z}$ on site 3 with the time $\tau$, the state becomes

$$|\phi_2''\rangle^\tau = e^{i\tau}\beta|\bar{x}_1\bar{x}_2 z_3 x_4 x_5 x_6\rangle - e^{i\tau}\mu|x_1 x_2 z_3 \bar{x}_4\bar{x}_5\bar{x}_6\rangle. \tag{90}$$

After the ITE operation of the Hamiltonian

$$H_3'' = -\sigma_1^x\sigma_2^x - \sigma_2^x\sigma_3^x - \sigma_4^x\sigma_5^x - \sigma_5^x\sigma_6^x, \tag{91}$$

the state becomes

$$|\phi_3''\rangle = \beta|\bar{x}_1\bar{x}_2\bar{x}_3 x_4 x_5 x_6\rangle - \mu|x_1 x_2 x_3\bar{x}_4\bar{x}_5\bar{x}_6\rangle. \tag{92}$$

Finally, the state is projected back to the ground-state space of the initial Hamiltonian

$$H_0 = -\sigma_1^x\sigma_2^x + \sigma_3^z - \sigma_4^x\sigma_5^x - \sigma_5^x\sigma_6^x, \tag{93}$$

and becomes

$$\begin{aligned}
|\phi_4''\rangle &= \beta|\bar{x}_1\bar{x}_2\bar{z}_3 x_4 x_5 x_6\rangle + \mu|x_1 x_2\bar{z}_3\bar{x}_4\bar{x}_5\bar{x}_6\rangle \\
&= (\beta-\mu)|0_{12}0_{456}\rangle|v_3\rangle + (\beta+\mu)|0_{12}1_{456}\rangle|v_3\rangle \\
&- (\beta+\mu)|1_{12}0_{456}\rangle|v_3\rangle - (\beta-\mu)|1_{12}1_{456}\rangle|v_3\rangle,
\end{aligned} \tag{94}$$

which is different from the final state without error

$$\begin{aligned}
|\phi_4\rangle &= e^{-i\tau}\alpha|x_1 x_2\bar{z}_3 x_4 x_5 x_6\rangle + e^{i\tau}\beta|\bar{x}_1\bar{x}_2\bar{z}_3 x_4 x_5 x_6\rangle + e^{i\tau}\mu|x_1 x_2\bar{z}_3\bar{x}_4\bar{x}_5\bar{x}_6\rangle + e^{-i\tau}\nu|\bar{x}_1\bar{x}_2\bar{z}_3\bar{x}_4\bar{x}_5\bar{x}_6\rangle, \\
&= (e^{-i\tau}\alpha + e^{i\tau}\beta - e^{i\tau}\mu - e^{-i\tau}\nu)|0_{12}0_{456}\rangle|v_3\rangle + (e^{-i\tau}\alpha + e^{i\tau}\beta + e^{i\tau}\mu + e^{-i\tau}\nu)|0_{12}1_{456}\rangle|v_3\rangle \\
&+ (e^{-i\tau}\alpha - e^{i\tau}\beta - e^{i\tau}\mu + e^{i\tau}\nu)|1_{12}0_{456}\rangle|v_3\rangle + (e^{-i\tau}\alpha - e^{i\tau}\beta + e^{i\tau}\mu - e^{-i\tau}\nu)|1_{12}1_{456}\rangle|v_3\rangle. \\
&= (e^{-i\tau}\alpha + e^{i\tau}\beta - e^{i\tau}\mu - e^{-i\tau}\nu)|00_g\rangle + (e^{-i\tau}\alpha + e^{i\tau}\beta + e^{i\tau}\mu + e^{-i\tau}\nu)|01_g\rangle \\
&+ (e^{-i\tau}\alpha - e^{i\tau}\beta - e^{i\tau}\mu + e^{i\tau}\nu)|10_g\rangle + (e^{-i\tau}\alpha - e^{i\tau}\beta + e^{i\tau}\mu - e^{-i\tau}\nu)|11_g\rangle.
\end{aligned} \tag{95}$$

### G. Effect of the flip errors between the nearest sites 4 and 5 during the phase gate

The influence of flip error perturbations in the Kitaev chain is significantly suppressed [31]. To study their effect in our simulator we consider the perturbation $c_k^\dagger c_{k+1} + c_{k+1}^\dagger c_k$,

which is a two site error, during the phase gate operation. This operator can be written in terms of spins as $(\sigma_k^y\sigma_{k+1}^y + \sigma_k^x\sigma_{k+1}^x)/2$. Similarly to the phase error the influence of the flip error dependents on the sites where the error happens. When the error only acts on at most one MZM, it can not influence the information encoded in the MZMs. To demonstrate this characteristic, we assume the error operates on sites 4 and 5 during the whole process of the gate operation.

The state evolution during the phase gate in the presence of flip errors on sites 4 and 5 is calculated as follows. After the ITE operation of the initial Hamiltonian

$$H_0 = -\sigma_1^x\sigma_2^x + \sigma_3^z - \sigma_4^x\sigma_5^x - \sigma_5^x\sigma_6^x, \tag{96}$$

the state becomes

$$|\phi_0\rangle = \alpha|x_1x_2\bar{z}_3x_4x_5x_6\rangle + \beta|\bar{x}_1\bar{x}_2\bar{z}_3x_4x_5x_6\rangle + \mu|x_1x_2\bar{z}_3\bar{x}_4\bar{x}_5\bar{x}_6\rangle + \nu|\bar{x}_1\bar{x}_2\bar{z}_3\bar{x}_4\bar{x}_5\bar{x}_6\rangle. \tag{97}$$

The flip error operation is then implemented and the state becomes

$$\begin{aligned}|\phi_0\rangle_{err} = &(\alpha|x_1x_2\bar{z}_3x_4x_5x_6\rangle + \beta|\bar{x}_1\bar{x}_2\bar{z}_3x_4x_5x_6\rangle + \mu|x_1x_2\bar{z}_3\bar{x}_4\bar{x}_5\bar{x}_6\rangle + \nu|\bar{x}_1\bar{x}_2\bar{z}_3\bar{x}_4\bar{x}_5\bar{x}_6\rangle)/2\\ &- (\alpha|x_1x_2\bar{z}_3\bar{x}_4\bar{x}_5x_6\rangle + \beta|\bar{x}_1\bar{x}_2\bar{z}_3\bar{x}_4\bar{x}_5x_6\rangle + \mu|x_1x_2\bar{z}_3x_4x_5\bar{x}_6\rangle + \nu|\bar{x}_1\bar{x}_2\bar{z}_3x_4x_5\bar{x}_6\rangle)/2.\end{aligned} \tag{98}$$

There is a probability of 0.5 that the states of particle 4 and 5 disturbed by the operation $\sigma_4^x\sigma_5^x$, and a probability of 0.5 disturbed by the operation $\sigma_4^y\sigma_5^y$. The state is then sent to the second ITE operation with the Hamiltonian

$$H_1'' = -\sigma_1^x\sigma_2^x - \sigma_2^x\sigma_3^x - \sigma_4^x\sigma_5^x - \sigma_5^x\sigma_6^x, \tag{99}$$

and becomes

$$|\phi_1''\rangle = \alpha|x_1x_2x_3x_4x_5x_6\rangle - \beta|\bar{x}_1\bar{x}_2\bar{x}_3x_4x_5x_6\rangle + \mu|x_1x_2x_3\bar{x}_4\bar{x}_5\bar{x}_6\rangle - \nu|\bar{x}_1\bar{x}_2\bar{x}_3\bar{x}_4\bar{x}_5\bar{x}_6\rangle. \tag{100}$$

The disturbed terms with the operation of $\sigma_4^y\sigma_5^y$ are discarded by the ITE of the Hamiltonian $-\sigma_5^x\sigma_6^x$. The flip error is further implemented and the state becomes

$$\begin{aligned}|\phi_1''\rangle_{err} = &(\alpha|x_1x_2x_3x_4x_5x_6\rangle - \beta|\bar{x}_1\bar{x}_2\bar{x}_3x_4x_5x_6\rangle + \mu|x_1x_2x_3\bar{x}_4\bar{x}_5\bar{x}_6\rangle - \nu|\bar{x}_1\bar{x}_2\bar{x}_3\bar{x}_4\bar{x}_5\bar{x}_6\rangle)/2\\ &- (\alpha|x_1x_2x_3\bar{x}_4\bar{x}_5x_6\rangle - \beta|\bar{x}_1\bar{x}_2\bar{x}_3\bar{x}_4\bar{x}_5x_6\rangle + \mu|x_1x_2x_3x_4x_5\bar{x}_6\rangle - \nu|\bar{x}_1\bar{x}_2\bar{x}_3x_4x_5\bar{x}_6\rangle)/2.\end{aligned} \tag{101}$$

The next ITE operation corresponds to the Hamiltonian

$$H_2'' = -\sigma_1^x\sigma_2^x + \sigma_2^x\sigma_3^z\sigma_4^x - \sigma_4^x\sigma_5^x - \sigma_5^x\sigma_6^x, \tag{102}$$

which leads to the state

$$|\phi_2''\rangle = \alpha|x_1x_2\bar{z}_3x_4x_5x_6\rangle - \beta|\bar{x}_1\bar{x}_2z_3x_4x_5x_6\rangle + \mu|x_1x_2z_3\bar{x}_4\bar{x}_5\bar{x}_6\rangle + \nu|\bar{x}_1\bar{x}_2\bar{z}_3\bar{x}_4\bar{x}_5\bar{x}_6\rangle. \tag{103}$$

The flip error operation is implemented and the state becomes

$$\begin{aligned}|\phi_2''\rangle_{err} = &(\alpha|x_1x_2\bar{z}_3x_4x_5x_6\rangle - \beta|\bar{x}_1\bar{x}_2z_3x_4x_5x_6\rangle + \mu|x_1x_2z_3\bar{x}_4\bar{x}_5\bar{x}_6\rangle + \nu|\bar{x}_1\bar{x}_2\bar{z}_3\bar{x}_4\bar{x}_5\bar{x}_6\rangle)/2\\ &- (\alpha|x_1x_2\bar{z}_3\bar{x}_4\bar{x}_5x_6\rangle - \beta|\bar{x}_1\bar{x}_2z_3\bar{x}_4\bar{x}_5x_6\rangle + \mu|x_1x_2z_3x_4x_5\bar{x}_6\rangle + \nu|\bar{x}_1\bar{x}_2\bar{z}_3x_4x_5\bar{x}_6\rangle)/2.\end{aligned} \tag{104}$$

By implementing the real time evolution of $e^{i\sigma_3^z\tau}$ on site 3 for time $\tau$, the state becomes

$$\begin{aligned}|\phi_2''\rangle^\tau = &(e^{-i\tau}\alpha|x_1x_2\bar{z}_3x_4x_5x_6\rangle - e^{i\tau}\beta|\bar{x}_1\bar{x}_2z_3x_4x_5x_6\rangle + e^{i\tau}\mu|x_1x_2z_3\bar{x}_4\bar{x}_5\bar{x}_6\rangle + e^{-i\tau}\nu|\bar{x}_1\bar{x}_2\bar{z}_3\bar{x}_4\bar{x}_5\bar{x}_6\rangle)/2\\ &- (e^{-i\tau}\alpha|x_1x_2\bar{z}_3\bar{x}_4\bar{x}_5x_6\rangle - e^{i\tau}\beta|\bar{x}_1\bar{x}_2z_3\bar{x}_4\bar{x}_5x_6\rangle + e^{i\tau}\mu|x_1x_2z_3x_4x_5\bar{x}_6\rangle + e^{-i\tau}\nu|\bar{x}_1\bar{x}_2\bar{z}_3x_4x_5\bar{x}_6\rangle)/2.\end{aligned} \tag{105}$$

The state then undergoes the ITE operation corresponding to the Hamiltonian

$$H_3'' = -\sigma_1^x\sigma_2^x - \sigma_2^x\sigma_3^x - \sigma_4^x\sigma_5^x - \sigma_5^x\sigma_6^x, \tag{106}$$

and becomes

$$|\phi_3''\rangle = e^{-i\tau}\alpha|x_1x_2x_3x_4x_5x_6\rangle - e^{i\tau}\beta|\bar{x}_1\bar{x}_2\bar{x}_3x_4x_5x_6\rangle + e^{i\tau}\mu|x_1x_2x_3\bar{x}_4\bar{x}_5\bar{x}_6\rangle - e^{-i\tau}\nu|\bar{x}_1\bar{x}_2\bar{x}_3\bar{x}_4\bar{x}_5\bar{x}_6\rangle. \tag{107}$$

The flip error operation is further implemented and the state becomes

$$\begin{aligned}|\phi_3''\rangle_{err} = &(e^{-i\tau}\alpha|x_1x_2x_3x_4x_5x_6\rangle - e^{i\tau}\beta|\bar{x}_1\bar{x}_2\bar{x}_3x_4x_5x_6\rangle + e^{i\tau}\mu|x_1x_2x_3\bar{x}_4\bar{x}_5\bar{x}_6\rangle - e^{-i\tau}\nu|\bar{x}_1\bar{x}_2\bar{x}_3\bar{x}_4\bar{x}_5\bar{x}_6\rangle)/2\\ &- (e^{-i\tau}\alpha|x_1x_2x_3\bar{x}_4\bar{x}_5x_6\rangle - e^{i\tau}\beta|\bar{x}_1\bar{x}_2\bar{x}_3\bar{x}_4\bar{x}_5x_6\rangle + e^{i\tau}\mu|x_1x_2x_3x_4x_5\bar{x}_6\rangle - e^{-i\tau}\nu|\bar{x}_1\bar{x}_2\bar{x}_3x_4x_5\bar{x}_6\rangle)/2.\end{aligned} \tag{108}$$

The state is then projected back to the ground-state space of the initial Hamiltonian

$$H_0 = -\sigma_1^x\sigma_2^x + \sigma_3^z - \sigma_4^x\sigma_5^x - \sigma_5^x\sigma_6^x, \tag{109}$$

and becomes

$$
\begin{aligned}
|\phi_4''\rangle &= e^{-i\tau}\alpha|x_1x_2\bar{z}_3x_4x_5x_6\rangle + e^{i\tau}\beta|\bar{x}_1\bar{x}_2\bar{z}_3x_4x_5x_6\rangle + e^{i\tau}\mu|x_1x_2\bar{z}_3\bar{x}_4\bar{x}_5\bar{x}_6\rangle + e^{-i\tau}\nu|\bar{x}_1\bar{x}_2\bar{z}_3\bar{x}_4\bar{x}_5\bar{x}_6\rangle, \\
&= (e^{-i\tau}\alpha + e^{i\tau}\beta - e^{i\tau}\mu - e^{-i\tau}\nu)|0_{12}0_{456}\rangle|v_3\rangle + (e^{-i\tau}\alpha + e^{i\tau}\beta + e^{i\tau}\mu + e^{-i\tau}\nu)|0_{12}1_{456}\rangle|v_3\rangle \\
&+ (e^{-i\tau}\alpha - e^{i\tau}\beta - e^{i\tau}\mu + e^{i\tau}\nu)|1_{12}0_{456}\rangle|v_3\rangle + (e^{-i\tau}\alpha - e^{i\tau}\beta + e^{i\tau}\mu - e^{-i\tau}\nu)|1_{12}1_{456}\rangle|v_3\rangle \\
&= (e^{-i\tau}\alpha + e^{i\tau}\beta - e^{i\tau}\mu - e^{-i\tau}\nu)|00_g\rangle + (e^{-i\tau}\alpha + e^{i\tau}\beta + e^{i\tau}\mu + e^{-i\tau}\nu)|01_g\rangle \\
&+ (e^{-i\tau}\alpha - e^{i\tau}\beta - e^{i\tau}\mu + e^{i\tau}\nu)|10_g\rangle + (e^{-i\tau}\alpha - e^{i\tau}\beta + e^{i\tau}\mu - e^{-i\tau}\nu)|11_g\rangle.
\end{aligned}
\tag{110}
$$

which is the same state as that without error. Hence, the system is fault-tolerant against flip error perturbations.

### H. Effect of flip errors between the nearest sites 3 and 4 during the phase gate

When the flip error $(\sigma_k^y\sigma_{k+1}^y + \sigma_k^x\sigma_{k+1}^x)/2$ acts on two or more MZMs the information encoded in the MZMs will be affected. To demonstrate this, we take the error to act on sites 3 and 4, when two MZMs are positioned on site 3, simultaneously. The state evolution during the phase gate with the flip error perturbation acting on sites 3 and 4 is calculated as follows.

After the ITE operation of the initial Hamiltonian

$$H_0 = -\sigma_1^x\sigma_2^x + \sigma_3^z - \sigma_4^x\sigma_5^x - \sigma_5^x\sigma_6^x, \tag{111}$$

the state becomes

$$|\phi_0\rangle = \alpha|x_1x_2\bar{z}_3x_4x_5x_6\rangle + \beta|\bar{x}_1\bar{x}_2\bar{z}_3x_4x_5x_6\rangle + \mu|x_1x_2\bar{z}_3\bar{x}_4\bar{x}_5\bar{x}_6\rangle + \nu|\bar{x}_1\bar{x}_2\bar{z}_3\bar{x}_4\bar{x}_5\bar{x}_6\rangle. \tag{112}$$

The state is then sent to the second ITE operation with the Hamiltonian

$$H_1'' = -\sigma_1^x\sigma_2^x - \sigma_2^x\sigma_3^x - \sigma_4^x\sigma_5^x - \sigma_5^x\sigma_6^x, \tag{113}$$

and becomes

$$|\phi_1''\rangle = \alpha|x_1x_2x_3x_4x_5x_6\rangle - \beta|\bar{x}_1\bar{x}_2\bar{x}_3x_4x_5x_6\rangle + \mu|x_1x_2x_3\bar{x}_4\bar{x}_5\bar{x}_6\rangle - \nu|\bar{x}_1\bar{x}_2\bar{x}_3\bar{x}_4\bar{x}_5\bar{x}_6\rangle. \tag{114}$$

The next ITE operation corresponds to the Hamiltonian

$$H_2'' = -\sigma_1^x\sigma_2^x + \sigma_2^x\sigma_3^z\sigma_4^x - \sigma_4^x\sigma_5^x - \sigma_5^x\sigma_6^x, \tag{115}$$

and the state becomes

$$|\phi_2''\rangle = \alpha|x_1x_2\bar{z}_3x_4x_5x_6\rangle - \beta|\bar{x}_1\bar{x}_2z_3x_4x_5x_6\rangle + \mu|x_1x_2z_3\bar{x}_4\bar{x}_5\bar{x}_6\rangle + \nu|\bar{x}_1\bar{x}_2\bar{z}_3\bar{x}_4\bar{x}_5\bar{x}_6\rangle. \quad (116)$$

The flip error operation is then implemented and the state becomes

$$\begin{aligned}|\phi_2''\rangle_{err} = &(\alpha|x_1x_2z_3x_4x_5x_6\rangle - \beta|\bar{x}_1\bar{x}_2\bar{z}_3x_4x_5x_6\rangle - \mu|x_1x_2\bar{z}_3\bar{x}_4\bar{x}_5\bar{x}_6\rangle - \nu|\bar{x}_1\bar{x}_2z_3\bar{x}_4\bar{x}_5\bar{x}_6\rangle)/2\\ &+ (-\alpha|x_1x_2z_3\bar{x}_4x_5x_6\rangle - \beta|\bar{x}_1\bar{x}_2\bar{z}_3\bar{x}_4x_5x_6\rangle - \mu|x_1x_2\bar{z}_3x_4\bar{x}_5\bar{x}_6\rangle + \nu|\bar{x}_1\bar{x}_2z_3x_4\bar{x}_5\bar{x}_6\rangle)/2.\end{aligned} \quad (117)$$

By implementing the real time evolution of $e^{i\sigma_3^z\tau}$ on site 3 with the time $\tau$, the state becomes

$$\begin{aligned}|\phi_2''\rangle^\tau = &(e^{i\tau}\alpha|x_1x_2z_3x_4x_5x_6\rangle - e^{-i\tau}\beta|\bar{x}_1\bar{x}_2\bar{z}_3x_4x_5x_6\rangle - e^{-i\tau}\mu|x_1x_2\bar{z}_3\bar{x}_4\bar{x}_5\bar{x}_6\rangle - e^{i\tau}\nu|\bar{x}_1\bar{x}_2z_3\bar{x}_4\bar{x}_5\bar{x}_6\rangle)/2\\ &+ (-e^{i\tau}\alpha|x_1x_2z_3\bar{x}_4x_5x_6\rangle - e^{-i\tau}\beta|\bar{x}_1\bar{x}_2\bar{z}_3\bar{x}_4x_5x_6\rangle - e^{-i\tau}\mu|x_1x_2\bar{z}_3x_4\bar{x}_5\bar{x}_6\rangle + e^{i\tau}\nu|\bar{x}_1\bar{x}_2z_3x_4\bar{x}_5\bar{x}_6\rangle)/2.\end{aligned} \quad (118)$$

The state then undergoes the ITE operation corresponding to the Hamiltonian

$$H_3'' = -\sigma_1^x\sigma_2^x - \sigma_2^x\sigma_3^x - \sigma_4^x\sigma_5^x - \sigma_5^x\sigma_6^x, \quad (119)$$

and becomes

$$|\phi_3''\rangle = e^{i\tau}\alpha|x_1x_2x_3x_4x_5x_6\rangle + e^{-i\tau}\beta|\bar{x}_1\bar{x}_2\bar{x}_3x_4x_5x_6\rangle - e^{-i\tau}\mu|x_1x_2x_3\bar{x}_4\bar{x}_5\bar{x}_6\rangle - e^{i\tau}\nu|\bar{x}_1\bar{x}_2\bar{x}_3\bar{x}_4\bar{x}_5\bar{x}_6\rangle. \quad (120)$$

The disturbed terms with the operation $\sigma_3^y\sigma_4^y$ are discarded by the ITE operation of $-\sigma_4^x\sigma_5^x$. The state is then projected back to the ground-state space of the initial Hamiltonian

$$H_0 = -\sigma_1^x\sigma_2^x + \sigma_3^z - \sigma_4^x\sigma_5^x - \sigma_5^x\sigma_6^x, \quad (121)$$

and becomes

$$\begin{aligned}|\phi_4''\rangle &= e^{i\tau}\alpha|x_1x_2\bar{z}_3x_4x_5x_6\rangle - e^{-i\tau}\beta|\bar{x}_1\bar{x}_2\bar{z}_3x_4x_5x_6\rangle - e^{-i\tau}\mu|x_1x_2\bar{z}_3\bar{x}_4\bar{x}_5\bar{x}_6\rangle + e^{i\tau}\nu|\bar{x}_1\bar{x}_2\bar{z}_3\bar{x}_4\bar{x}_5\bar{x}_6\rangle,\\ &= (e^{i\tau}\alpha - e^{-i\tau}\beta - e^{-i\tau}\mu + e^{i\tau}\nu)|0_{12}0_{456}\rangle|v_3\rangle + (e^{i\tau}\alpha - e^{-i\tau}\beta + e^{-i\tau}\mu - e^{i\tau}\nu)|0_{12}1_{456}\rangle|v_3\rangle\\ &+ (e^{i\tau}\alpha + e^{-i\tau}\beta - e^{-i\tau}\mu - e^{i\tau}\nu)|1_{12}0_{456}\rangle|v_3\rangle + (e^{i\tau}\alpha + e^{-i\tau}\beta + e^{-i\tau}\mu + e^{i\tau}\nu)|1_{12}1_{456}\rangle|v_3\rangle\\ &= (e^{i\tau}\alpha - e^{-i\tau}\beta - e^{-i\tau}\mu + e^{i\tau}\nu)|00_g\rangle + (e^{i\tau}\alpha - e^{-i\tau}\beta + e^{-i\tau}\mu - e^{i\tau}\nu)|01_g\rangle\\ &+ (e^{i\tau}\alpha + e^{-i\tau}\beta - e^{-i\tau}\mu - e^{i\tau}\nu)|10_g\rangle + (e^{i\tau}\alpha + e^{-i\tau}\beta + e^{-i\tau}\mu + e^{i\tau}\nu)|11_g\rangle.\end{aligned} \quad (122)$$

This state is different from the state obtained in the absence of errors, given by

$$
\begin{aligned}
|\phi_4''\rangle &= e^{-i\tau}\alpha|x_1x_2\bar{z}_3x_4x_5x_6\rangle + e^{i\tau}\beta|\bar{x}_1\bar{x}_2\bar{z}_3x_4x_5x_6\rangle + e^{i\tau}\mu|x_1x_2\bar{z}_3\bar{x}_4\bar{x}_5\bar{x}_6\rangle + e^{-i\tau}\nu|\bar{x}_1\bar{x}_2\bar{z}_3\bar{x}_4\bar{x}_5\bar{x}_6\rangle, \\
&= (e^{-i\tau}\alpha + e^{i\tau}\beta - e^{i\tau}\mu - e^{-i\tau}\nu)|0_{12}0_{456}\rangle|v_3\rangle + (e^{-i\tau}\alpha + e^{i\tau}\beta + e^{i\tau}\mu + e^{-i\tau}\nu)|0_{12}1_{456}\rangle|v_3\rangle \\
&+ (e^{-i\tau}\alpha - e^{i\tau}\beta - e^{i\tau}\mu + e^{i\tau}\nu)|1_{12}0_{456}\rangle|v_3\rangle + (e^{-i\tau}\alpha - e^{i\tau}\beta + e^{i\tau}\mu - e^{-i\tau}\nu)|1_{12}1_{456}\rangle|v_3\rangle \\
&= (e^{-i\tau}\alpha + e^{i\tau}\beta - e^{i\tau}\mu - e^{-i\tau}\nu)|00_g\rangle + (e^{-i\tau}\alpha + e^{i\tau}\beta + e^{i\tau}\mu + e^{-i\tau}\nu)|01_g\rangle \\
&+ (e^{-i\tau}\alpha - e^{i\tau}\beta - e^{i\tau}\mu + e^{i\tau}\nu)|10_g\rangle + (e^{-i\tau}\alpha - e^{i\tau}\beta + e^{i\tau}\mu - e^{-i\tau}\nu)|11_g\rangle.
\end{aligned}
\tag{123}
$$

The transformation can be written as

$$
U' = \begin{pmatrix}
i\sin\tau & 0 & 0 & \cos\tau \\
0 & i\sin\tau & \cos\tau & 0 \\
0 & \cos\tau & i\sin\tau & 0 \\
\cos\tau & 0 & 0 & i\sin\tau
\end{pmatrix}. \tag{124}
$$

## I. Cross section images for the state evolution

The cross sections of the output spatial modes of each process in the exchanging of MZMs A and C are shown in Fig. S7. The solid rings represent the preserved optical modes, and the dashed rings represent the discarded optical modes. The states indicated next to the optical modes represent the corresponding basis of the preserved states.

In order to clearly illustrate the roles of BDs, the cross sections after each BDs during the basis rotation in Fig. S7 are shown in Fig. S8.

The cross sections of the output spatial modes of each process in the exchanging of MZMs C and D are shown in Fig. S9. The solid rings represent the preserved optical modes, and the dashed rings represent the discarded ones. The states indicated next to the optical modes represent the basis of the preserved states.

The cross sections of the output spatial modes of each process in the implementation of the $\frac{\pi}{8}$-phase gate are shown in Fig. S10. The solid rings represent the preserved optical modes and the dashed rings represent the discarded ones. The states indicated next to the optical modes represent the corresponding basis of the preserved states.

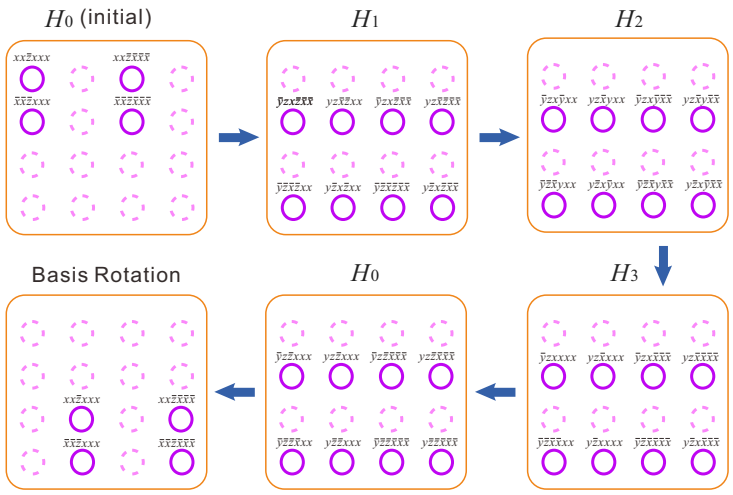


Fig. S7. Spatial modes of the output states for the exchange of MZMs A and C. The solid rings represent the preserved optical modes, and the dashed rings represent the discarded ones. The states indicated next to the optical modes represent the corresponding basis of the preserved modes.

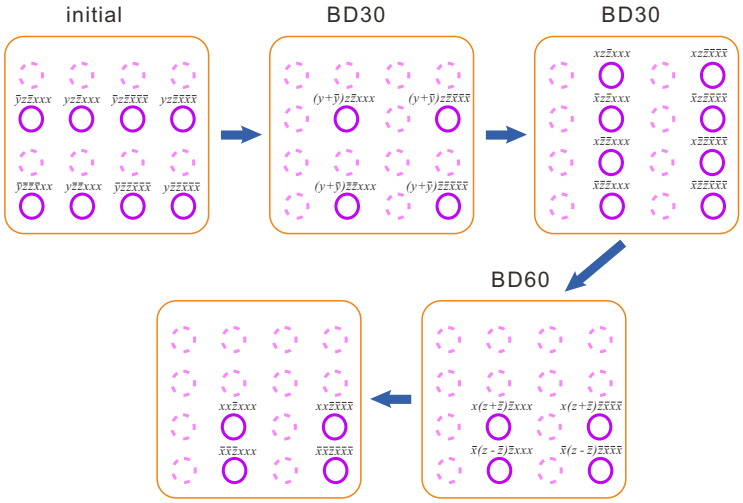


Fig. S8. Spatial modes of the output states corresponding to the basis rotation. The solid rings represent the preserved optical modes, and the dashed rings represent the discarded ones. BD30 and BD60 represent the beam displacers with beam displacement of 3.0 mm and 6.0 mm, respectively. The states indicated next to the optical modes represent the corresponding basis of the preserved modes.

## J. Realisation of the Deutsch-Jozsa algorithm based on Majorana braiding

We now explain how to implement the Deutsch-Jozsa algorithm with MZMs. The initial state (ground state of $H_0$) is given by

$$\begin{aligned}|\phi_0\rangle = (\alpha+\beta-\mu-\nu)|00_g\rangle + (\alpha+\beta+\mu+\nu)|01_g\rangle \\ + (\alpha-\beta-\mu+\nu)|10_g\rangle + (\alpha-\beta+\mu-\nu)|11_g\rangle.\end{aligned} \tag{125}$$

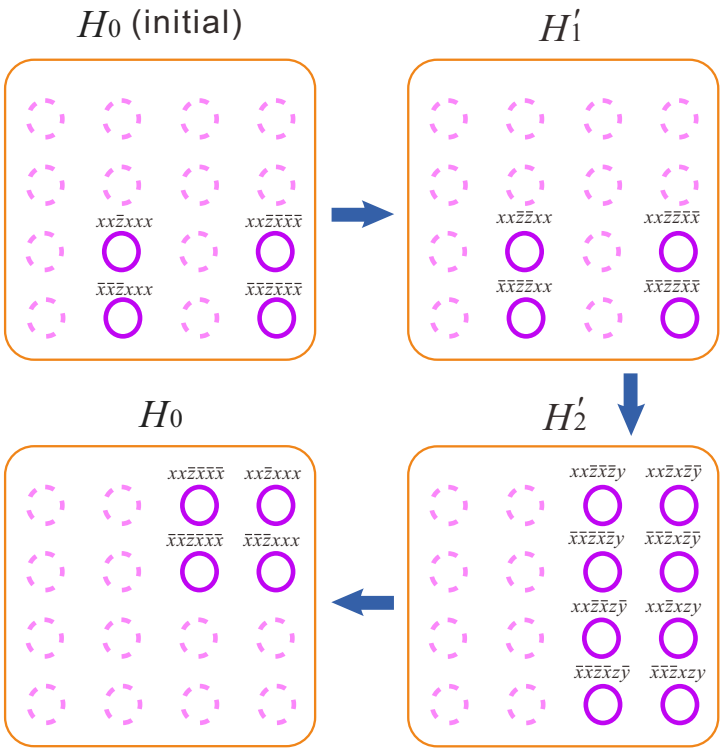


Fig. S9. Spatial modes of the output states for the exchange of MZMs C and D. The solid rings represent the preserved optical modes, and the dashed rings represent the discarded ones. The states indicated next to the optical modes represent the basis of the preserved states.

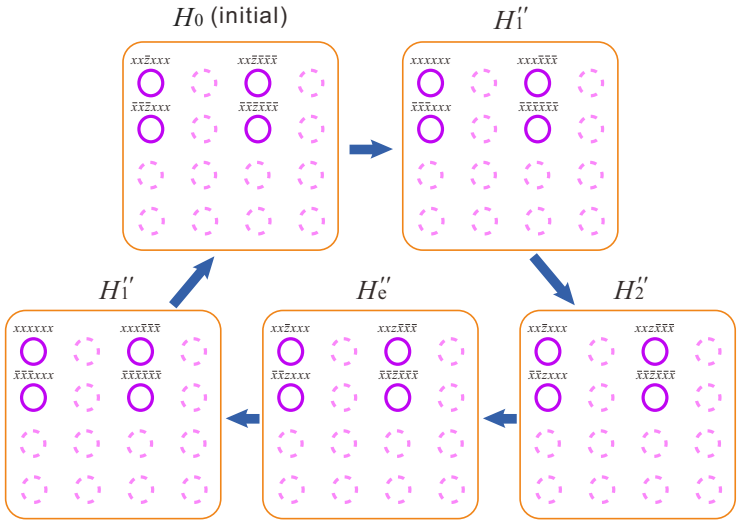


Fig. S10. Spatial modes of the output states for the $\frac{\pi}{8}$-phase operation. The solid rings represent the preserved optical modes and the dashed rings represent the discarded ones. The states indicated next to the optical modes represent the corresponding basis of the preserved states.

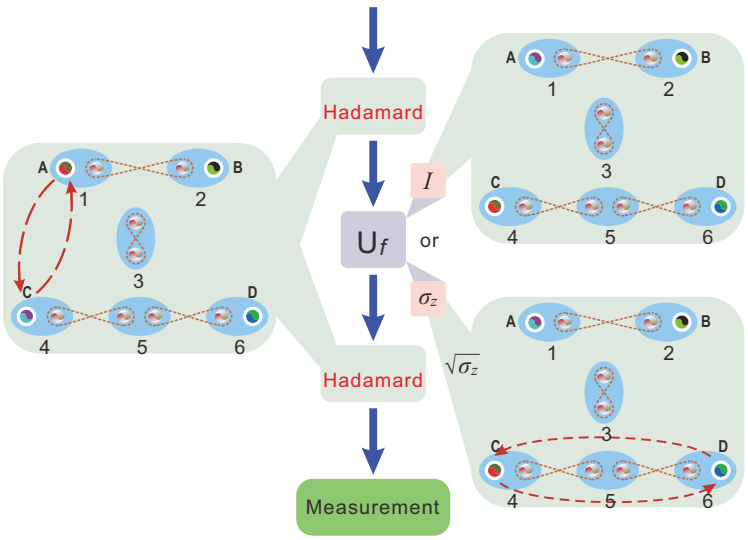


Fig. S11. The process to implement the Deutsch-Jozsa algorithm with the braiding of MZMs. The Hadamard gate is implemented by braiding A and C. For the unitary operation ($U_f$), the state remains the same when the operation is the identity (corresponding to constant function). Two successive braiding of C and D will be implemented when the operation is $\sigma_z$ (corresponding to balance function). Another Hadamard gate is implemented again after $U_f$. The final state is then measured.

After the braiding of MZMs A and C, the final state becomes

$$\begin{aligned} |\phi_4\rangle = (\beta-\mu)|00_g\rangle + (\beta+\mu)|01_g\rangle \\ + (\alpha+\nu)|10_g\rangle + (\alpha-\nu)|11_g\rangle. \end{aligned} \tag{126}$$

The unitary transformation reads

$$U = \frac{1}{\sqrt{2}} \begin{pmatrix} 1 & 0 & 0 & -1 \\ 0 & 1 & -1 & 0 \\ 0 & 1 & 1 & 0 \\ 1 & 0 & 0 & 1 \end{pmatrix}. \tag{127}$$

If we focus on the even fermionic parity state-space spanned by $|00_g\rangle$ and $|11_g\rangle$, the unitary transformation becomes

$$U = \frac{1}{\sqrt{2}} \begin{pmatrix} 1 & -1 \\ 1 & 1 \end{pmatrix}. \tag{128}$$

As a result, the braiding of A and C corresponds to a Hadamard gate operation on the basis of $|00_g\rangle$ and $|11_g\rangle$.

On the other hand, the braiding of the MZMs C and D acting on the initial state $|\phi_0\rangle$ gives

$$\begin{aligned} |\phi_2'\rangle = i(\alpha+\beta-\mu-\nu)|00_g\rangle + (\alpha+\beta+\mu+\nu)|01_g\rangle \\ + i(\alpha-\beta-\mu+\nu)|10_g\rangle + (\alpha-\beta+\mu-\nu)|11_g\rangle. \end{aligned} \tag{129}$$

This unitary operation, when restricted on the space of $|00_g\rangle$ and $|11_g\rangle$, it reads

$$U' = \begin{pmatrix} 1 & 0 \\ 0 & -i \end{pmatrix}. \tag{130}$$

Two successive operations of $U'$ give

$$\sigma_z = U'U' = \begin{pmatrix} 1 & 0 \\ 0 & -1 \end{pmatrix}. \tag{131}$$

As a result, two successive braidings of C and D MZMs correspond to the $\sigma_z$ operation on the basis of $|00_g\rangle$ and $|11_g\rangle$.

We can then implement the Deutsch-Jozsa algorithm in the space spanned by $|00_g\rangle$ and $|11_g\rangle$ and the detailed process is shown below:

1. We prepare the initial state $|00_g\rangle$ $(\frac{1}{2}(|x_1x_2\bar{z}_3x_4x_5x_6\rangle+|\bar{x}_1\bar{x}_2\bar{z}_3x_4x_5x_6\rangle-|x_1x_2\bar{z}_3\bar{x}_4\bar{x}_5\bar{x}_6\rangle-|\bar{x}_1\bar{x}_2\bar{z}_3\bar{x}_4\bar{x}_5\bar{x}_6\rangle))$.

2. After the exchange of A and C, the state becomes $\frac{1}{\sqrt{2}}(|00_g\rangle+|11_g\rangle)$ $(\frac{1}{\sqrt{2}}(|x_1x_2\bar{z}_3x_4x_5x_6\rangle-|\bar{x}_1\bar{x}_2\bar{z}_3\bar{x}_4\bar{x}_5\bar{x}_6\rangle))$.

3. If the function is constant, the state remains $\frac{1}{\sqrt{2}}(|00_g\rangle + |11_g\rangle)$ $(\frac{1}{\sqrt{2}}(|x_1x_2\bar{z}_3x_4x_5x_6\rangle - |\bar{x}_1\bar{x}_2\bar{z}_3\bar{x}_4\bar{x}_5\bar{x}_6\rangle))$.

4. We exchange A and C again, the state becomes $|11_g\rangle$ $(\frac{1}{2}(|x_1x_2\bar{z}_3x_4x_5x_6\rangle-|\bar{x}_1\bar{x}_2\bar{z}_3x_4x_5x_6\rangle+|x_1x_2\bar{z}_3\bar{x}_4\bar{x}_5\bar{x}_6\rangle - |\bar{x}_1\bar{x}_2\bar{z}_3\bar{x}_4\bar{x}_5\bar{x}_6\rangle))$.

5. If the function is balanced, the state undergoes two success exchange C and D. After the first exchange of C and D, the state becomes $\frac{1}{\sqrt{2}}(|00_g\rangle - i|11_g\rangle)$ $(\frac{1}{2}(|x_1x_2\bar{z}_3x_4x_5x_6\rangle + i|\bar{x}_1\bar{x}_2\bar{z}_3x_4x_5x_6\rangle - i|x_1x_2\bar{z}_3\bar{x}_4\bar{x}_5\bar{x}_6\rangle - |\bar{x}_1\bar{x}_2\bar{z}_3\bar{x}_4\bar{x}_5\bar{x}_6\rangle))$.

6. After the second exchange C and D, the state becomes $\frac{1}{\sqrt{2}}(|00_g\rangle-|11_g\rangle)$ $(\frac{1}{\sqrt{2}}(|x_1x_2\bar{z}_3\bar{x}_4\bar{x}_5\bar{x}_6\rangle-|\bar{x}_1\bar{x}_2\bar{z}_3x_4x_5x_6\rangle))$.

7. We then exchange A and C again and the state becomes $|00_g\rangle$ $(\frac{1}{2}(|x_1x_2\bar{z}_3x_4x_5x_6\rangle + |\bar{x}_1\bar{x}_2\bar{z}_3x_4x_5x_6\rangle - |x_1x_2\bar{z}_3\bar{x}_4\bar{x}_5\bar{x}_6\rangle - |\bar{x}_1\bar{x}_2\bar{z}_3\bar{x}_4\bar{x}_5\bar{x}_6\rangle))$.

As a result, we can distinguish constant and balanced function by only one measurement. If the outcome of the measurement is $|00_g\rangle$, the function is balanced. If the outcome is $|11_g\rangle$, the function is constant. The procedure that implements the Deutsch-Jozsa algorithm based on the braiding of MZMs is shown in Fig. S11.

## Section S2. Experimental details

### A. The experimental setup for the exchange of C and D MZMs

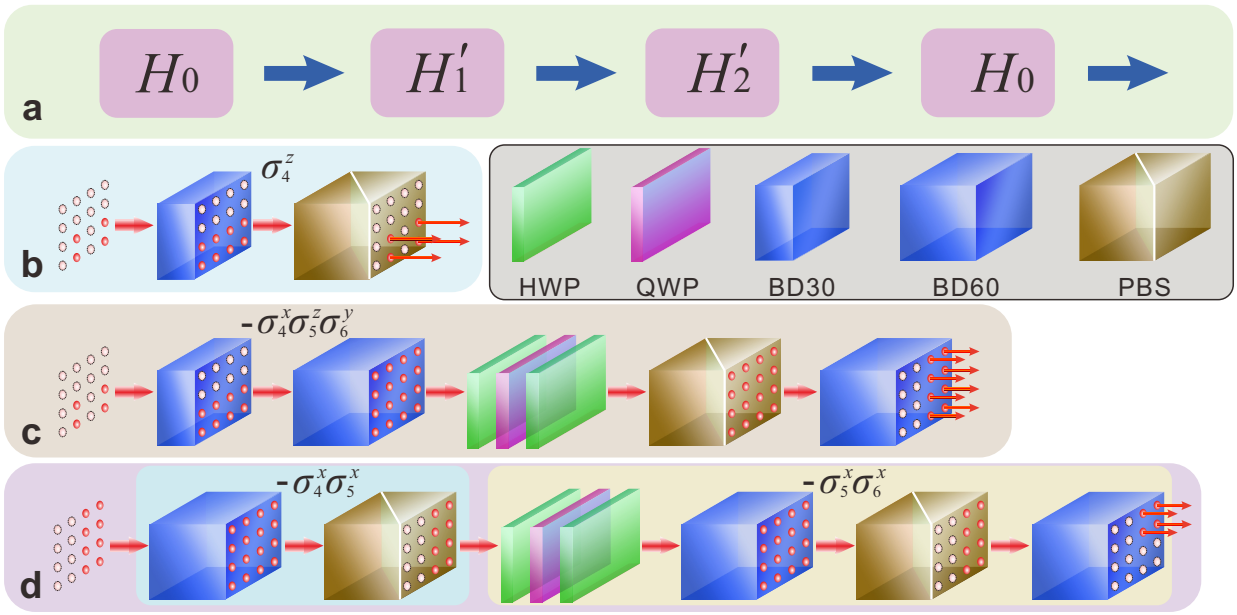


Fig. S12. Experimental setup for the exchange of MZMs C and D. **a.** The imaginary-time evolutions (ITEs) of the involved Hamiltonians to exchange MZMs C and D. **b.** The setup to realize the ITE of $H_1'$ (needed only the term of $\sigma_4^z$). The state is initially prepared to be the ground state of $H_0$ involving four spatial modes, which are represented by the solid circles. After transferred by a beam displacer (BD30 with beams separated by 3.0 mm) with half-wave plates (HWPs) operating on different spatial modes (not shown and the total operation is denoted as an thick arrow), and dissipated by a polarization beam splitter (PBS), the output state remains four spatial modes. **c.** The setup for the subsequent ITE of $H_2'$ (needed only the term of $-\sigma_4^x\sigma_5^z\sigma_6^y$). The combination of HWPs and a quarter-wave plate (QWP) is used to rotate the basis to the right-hand and left-hand circular basis. The beam displacers with beams separated by 6.0 mm (BD60s) are used to operate more spatial modes. **d.** The setup for the ITE of final $H_0$ (needed only the terms of $-\sigma_4^x\sigma_5^x$ and $-\sigma_5^x\sigma_6^x$).

The experimental setup for the exchange of C and D is shown in Fig. S12. The state information is prepared by beam displacers with beams separated by 3.0 mm (BD30) and with beams separated by 6.0 mm (BD60). The coupling between the spatial modes and the polarisation is achieved using half-wave plates (HWPs), which rotate the polarisation in the corresponding paths. Such a process is denoted by a thick arrow in the setup. The combination of HWPs and a quarter-wave plate (QWP) can be used to rotate the basis to the right-hand and left-hand circular basis, which exchanges the basis between $\sigma^y$ and $\sigma^x$ ($\sigma^z$). The dissipative evolution is achieved by passing the photons through a polarisation beam splitter (PBS), which transmits the horizontal component and reflects the vertical one. In our cases, only photons in the optical modes that have horizontal polarisations are preserved.

These modes correspond to the ground states of the Hamiltonian. The components with vertical polarisations are completely dissipated. We directly prepare the ground states of $H_0$ with the output state involving four spatial modes. The state is then sent to the ITE operation of $H_1'$, $H_2'$ and $H_0$ for implementing the braiding of MZMs C and D.

## B. The experimental setup for the implementation of $\pi/8$-phase gate and the error operations

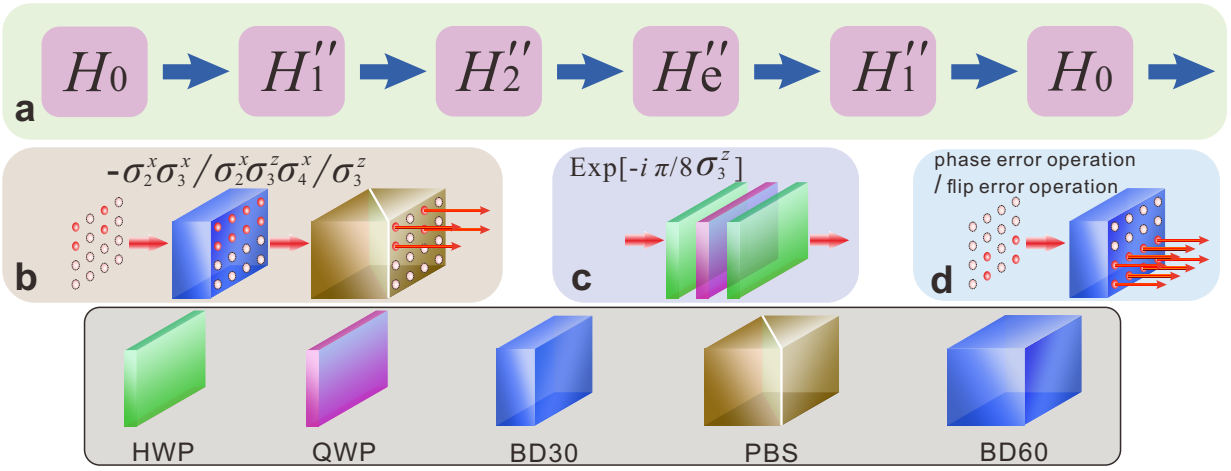


Fig. S13. Experimental setup for the implementation of $\frac{\pi}{8}$-phase gate and error operations. **a.** The imaginary-time evolutions (ITEs) of the involved Hamiltonians to exchange MZMs C and D. **b.** The setup to realize the ITE of $H_1''$ (needed only the term of $-\sigma_2^x\sigma_3^x$). The state is initially prepared to be the ground state of $H_0$ involving four spatial modes, which are represented by the solid circles. After transferred by a beam displacer (BD30 with beams separated by 3.0 mm) with half-wave plates (HWPs) operating on different spatial modes (not shown and the total operation is denoted as an thick arrow), and dissipated by a polarization beam splitter (PBS), the output state remains four spatial modes. The ITE setups of $H_2''$ (needed only the term of $\sigma_2^x\sigma_3^z\sigma_4^x$), the second $H_1''$ (needed only the term of $-\sigma_2^x\sigma_3^x$) and the second $H_0$ (needed only the term of $\sigma_3^z$) are similar to that of $H_1''$ with different operation of HWPs. **c.** The combination of HWPs and a quarter-wave plate (QWP) is used to realize the real time evolution of $H_e''$ with the operation as $e^{-i\pi/8\sigma_3^z}$. **d.** The setup to implement the phase error with the operation of $(1+\sigma^z)/2$ and the flip error with the operation of $(\sigma^y\sigma^y+\sigma^x\sigma^x)/2$. Four of the eight output modes are preserved, which corresponding to ITE operation of next Hamiltonian (not shown in the figure)

The experimental setup for the implementation of $\pi/8$ phase gate is shown in Fig. S13. The thick arrows between the optical components represent the coupling between the polarisation and spatial modes by implementing half-wave plates (HWPs) on different spatial modes. The ITE setups of $H_1''$, $H_2''$, the second $H_1''$ and the second $H_0$ are similar, which is shown in Fig. S13b. The combination of HWPs and a quarter-wave plate (QWP) is used to realize the real time evolution of $H_e''$, which is shown in Fig. S13c. The setups to im-

plement the phase error with the operation of $(1+\sigma^z)/2$ and flip error with the operation of $(\sigma^y\sigma^y+\sigma^x\sigma^x)/2$ are similar, which is shown in Fig. S13d. The phase error on site 4 is implemented during the gate manipulation, while the flip error on sites (4, 5) and sites (3, 4) is implemented when both MZMs are positioned on site 3 (after the ITE operation of $H_2''$). Only four of the eight output modes are preserved after the error operation, which is due to the ITE operation of the next Hamiltonian (not shown in the figure). The detailed analysis can be found in sections ID-G.

### C. The experimental setup for quantum process tomography

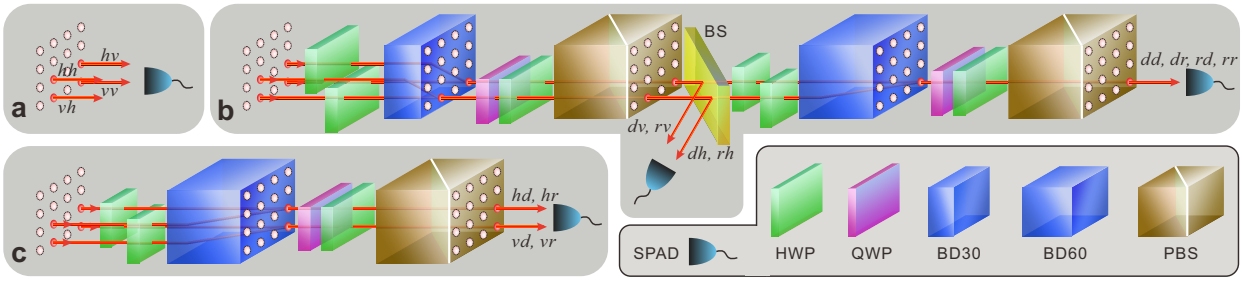


Fig. S14. Experimental setup for the quantum process tomography. The final gate operations are reconstructed through the quantum process tomography. Beam splitters (BSs) are used to send the photons to different measurement instruments. Different beam splitters (BD30 with beams separated by 3.0 mm and BD60 with beams separated by 6.0 mm) are used to reconstruct the interference between different spatial modes. Half-wave plates (HWPs), quarter-wave plates (QWPs) and polarisation beam splitters (PBS) are used to rotate different bases. $h$, $v$, $r$ and $d$ represent the horizontal polarisation, vertical polarisation, right-hand circular polarisation and diagonal polarisation, respectively. Finally, photons are detected using single-photon avalanche detectors (SPADs). **a.** is used to detect the photons in the basis of $\{hh, hv, vh, vv\}$. **b.** is used to detect the photons in the basis of $\{dr, rv, dh, rh\}$ and $\{dd, dr, rd, rr\}$. **c.** is used to detect the photons in the basis of $\{hd, hr, vd, vr\}$.

In our experiment, we perform the quantum process tomography to reconstruct the operations of different gates [34]. The experimental measurement basis is chosen to be $\{hh, hv, vh, vv\}$. $h$, $v$, $r$ and $d$ represent the horizontal polarisation, vertical polarisation, right-hand circular polarisation and diagonal polarisation, respectively. For each input state, we need to reconstruct the final output state by two-qubit-state tomography with 16 measurement configurations, as shown in Fig. S14**a**, **b** and **c**. To reconstruct the quantum process, we need 16 different input states.

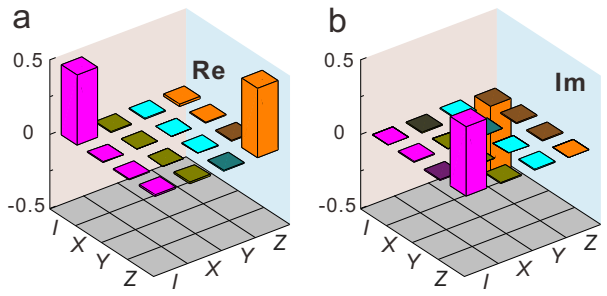


Fig. S15. Experimental density matrices resulting from the $(-\frac{\pi}{4})$-phase gate operation. The measurement basis of I, X, Y and Z represent the identity, $\sigma^x$, $\sigma^y$ and $\sigma^z$ operators, respectively. **a.** Real (Re) and **b.** Imaginary (Im) parts of the $(-\frac{\pi}{4})$-phase gate operator.

### D. More experimental results

The real and imaginary parts of the experimentally obtained density matrices of the $(-\frac{\pi}{4})$-phase gate expressed in the logical basis $\{|00_g\rangle, |11_g\rangle\}$ are shown in Figs. S15a and b. The experimental fidelity is $93.44 \pm 0.01\%$. The final density matrices obtained after the action of the gate operators in the basis $\{|00_g\rangle, |01_g\rangle, |10_g\rangle, |11_g\rangle\}$ are shown in Fig. S16. The density matrix in the basis $\{|00_g\rangle, |01_g\rangle, |10_g\rangle, |11_g\rangle\}$ obtained after the application of the $\frac{\pi}{8}$-phase gate in the presence of different errors, is shown in Fig. S17.

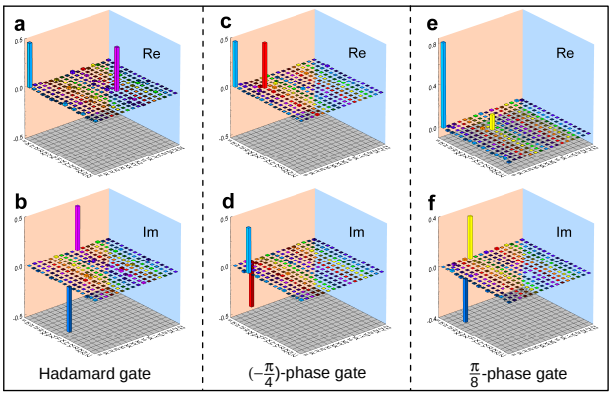


Fig. S16. Experimental density matrices resulting from the gate operations in the full basis. **a.** Real (Re) and **b.** Imaginary (Im) parts of the Hadamard gate operation. **c.** Real (Re) and **d.** Imaginary (Im) parts of the $(-\frac{\pi}{4})$-phase gate operation. **e.** Real (Re) and **f.** Imaginary (Im) parts of the $\frac{\pi}{8}$-phase gate operation.

We can demonstrate the Deutsch-Jozsa algorithm with the corresponding gates following the process described in section IJ. First we prepare the input state $|00_g\rangle$. If the operation in the box is the identity (constant function), the braiding operation of $U_{\mathrm{AC}}$ (braiding MZMs A and C) is implemented twice directly on the input state. The final state can

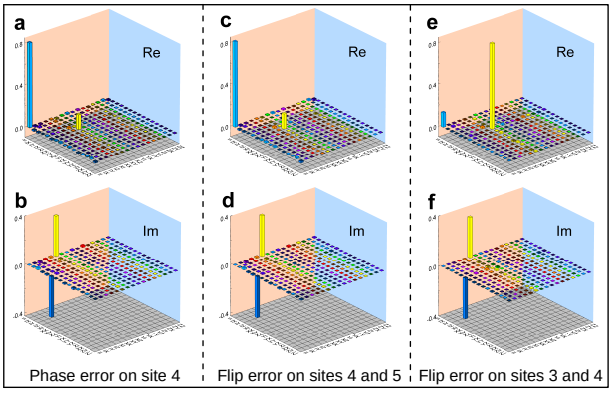


Fig. S17. Experimental density matrices resulting from the $\frac{\pi}{8}$-phase gate in the full basis. **a.** Real (Re) and **b.** Imaginary (Im) parts of the $\frac{\pi}{8}$-phase gate operation with phase error on site 4. **c.** Real (Re) and **d.** Imaginary (Im) parts of the $\frac{\pi}{8}$-phase gate operation with flip error on sites 4 and 5. **e.** Real (Re) and **f.** Imaginary (Im) parts of the $\frac{\pi}{8}$-phase gate operation with flip error on sites 3 and 4.

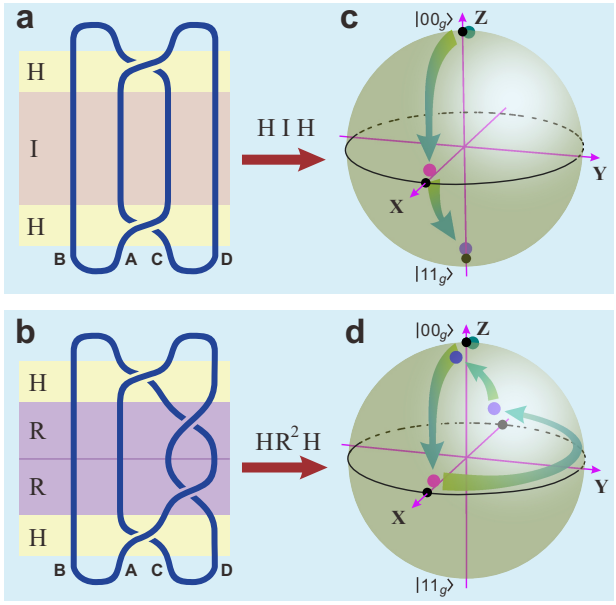


Fig. S18. The state evolution in the Deutsch-Jozsa algorithm. The state evolutions in the Deutsch-Jozsa algorithm with the initial state of $|00_g\rangle$ are shown in **c** (Identity operation) and **d** ($\sigma^z$ operation). Black dots are the theoretical predictions and coloured dots are the corresponding experimental results. The braiding patterns of the four MZMs A, B, C and D that correspond to the implementation of the Deutsch-Jozsa algorithm with $U_f$ being the identity or the $\sigma^z$ operation are shown in **a.** and **b.**, respectively.

be written as $U_{\mathrm{AC}}U_{\mathrm{AC}}|00_g\rangle = |11_g\rangle$, which corresponds to implementing the $\mathrm{H}\cdot\mathrm{I}\cdot\mathrm{H}$ gate operations. If the operation in the box is $\sigma^z$ (balanced function), the final state becomes $U_{\mathrm{AC}}U_{\mathrm{CD}}U_{\mathrm{CD}}U_{\mathrm{AC}}|00_g\rangle = |00_g\rangle$, where $U_{\mathrm{CD}}$ corresponds to the braiding of C and D. These gate operations can be written as $\mathrm{H}\cdot\mathrm{R}^2\cdot\mathrm{H}$. In this work, the output states, denoted as $\rho_c^e$ and $\rho_b^e$ for constant and balanced operations, respectively, are directly calculated from

the experimentally reconstructed operators $U_{\mathrm{AC}}$ and $U_{\mathrm{CD}}$. The state evolution during the operation of the Deutsch-Jozsa algorithm are shown in Figs. S18c and d, where the black dots and the coloured dots represent the corresponding theoretical and experimental results, respectively. The corresponding braiding patterns with isolated MZMs A, B, C, and D are shown in Figs. S18a and b. The final state fidelities are all very high, above 96%. The demonstrated Deutsch-Josza algorithm show what is possible to do with the gates obtained by the braiding of the MZMs and what the expected error would be.